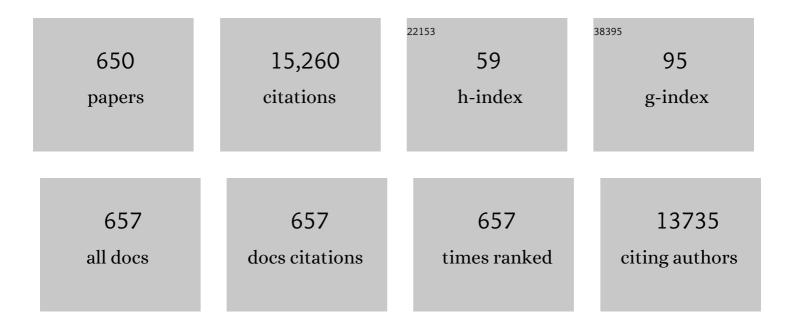
Gilles Patriarche

List of Publications by Year in descending order

Source: https://exaly.com/author-pdf/4271178/publications.pdf Version: 2024-02-01



#	Article	IF	CITATIONS
1	Why Does Wurtzite Form in Nanowires of III-V Zinc Blende Semiconductors?. Physical Review Letters, 2007, 99, 146101.	7.8	669
2	Core/Shell Colloidal Semiconductor Nanoplatelets. Journal of the American Chemical Society, 2012, 134, 18591-18598.	13.7	323
3	Band Alignment and Minigaps in Monolayer MoS ₂ -Graphene van der Waals Heterostructures. Nano Letters, 2016, 16, 4054-4061.	9.1	288
4	Analysis of vapor-liquid-solid mechanism in Au-assisted GaAs nanowire growth. Applied Physics Letters, 2005, 87, 203101.	3.3	249
5	Crystal Phase Quantum Dots. Nano Letters, 2010, 10, 1198-1201.	9.1	233
6	Efficient Exciton Concentrators Built from Colloidal Core/Crown CdSe/CdS Semiconductor Nanoplatelets. Nano Letters, 2014, 14, 207-213.	9.1	224
7	Height dispersion control of InAs/InP quantum dots emitting at 1.55 μm. Applied Physics Letters, 2001, 78, 1751-1753.	3.3	164
8	From Excitonic to Photonic Polariton Condensate in a ZnO-Based Microcavity. Physical Review Letters, 2013, 110, 196406.	7.8	162
9	Predictive modeling of self-catalyzed III-V nanowire growth. Physical Review B, 2013, 88, .	3.2	158
10	van der Waals Epitaxy of GaSe/Graphene Heterostructure: Electronic and Interfacial Properties. ACS Nano, 2016, 10, 9679-9686.	14.6	154
11	Type-II CdSe/CdTe Core/Crown Semiconductor Nanoplatelets. Journal of the American Chemical Society, 2014, 136, 16430-16438.	13.7	153
12	Infrared Photodetection Based on Colloidal Quantum-Dot Films with High Mobility and Optical Absorption up to THz. Nano Letters, 2016, 16, 1282-1286.	9.1	150
13	Ultra-low-threshold continuous-wave and pulsed lasing in tensile-strained GeSn alloys. Nature Photonics, 2020, 14, 375-382.	31.4	145
14	Gradient CdSe/CdS Quantum Dots with Room Temperature Biexciton Unity Quantum Yield. Nano Letters, 2015, 15, 3953-3958.	9.1	143
15	Au-assisted molecular beam epitaxy of InAs nanowires: Growth and theoretical analysis. Journal of Applied Physics, 2007, 102, 094313.	2.5	136
16	Silicon Nanowires Coated with Silver Nanostructures as Ultrasensitive Interfaces for Surface-Enhanced Raman Spectroscopy. ACS Applied Materials & Interfaces, 2009, 1, 1396-1403.	8.0	133
17	Arsenic Pathways in Self-Catalyzed Growth of GaAs Nanowires. Crystal Growth and Design, 2013, 13, 91-96.	3.0	133
18	Protein Transport through a Narrow Solid-State Nanopore at High Voltage: Experiments and Theory. ACS Nano, 2012, 6, 6236-6243.	14.6	126

#	Article	IF	CITATIONS
19	Sub-5nm FIB direct patterning of nanodevices. Microelectronic Engineering, 2007, 84, 779-783.	2.4	117
20	Synthesis and optical characterizations of Yb-doped CaF2 ceramics. Optical Materials, 2009, 31, 750-753.	3.6	113
21	Atomic Step Flow on a Nanofacet. Physical Review Letters, 2018, 121, 166101.	7.8	113
22	Growth and Characterization of Wurtzite GaAs Nanowires with Defect-Free Zinc Blende GaAsSb Inserts. Nano Letters, 2008, 8, 4459-4463.	9.1	112
23	New progresses in transparent rare-earth doped glass-ceramics. Optical Materials, 2001, 16, 255-267.	3.6	110
24	Synthesis and optical characterizations of undoped and rare-earth-doped CaF2 nanoparticles. Journal of Solid State Chemistry, 2006, 179, 2636-2644.	2.9	110
25	Growth and Characterization of InP Nanowires with InAsP Insertions. Nano Letters, 2007, 7, 1500-1504.	9.1	110
26	Growth of GaN free-standing nanowires by plasma-assisted molecular beam epitaxy: structural and optical characterization. Nanotechnology, 2007, 18, 385306.	2.6	109
27	Temperature conditions for GaAs nanowire formation by Au-assisted molecular beam epitaxy. Nanotechnology, 2006, 17, 4025-4030.	2.6	107
28	Colloidal CdSe/CdS Dot-in-Plate Nanocrystals with 2D-Polarized Emission. ACS Nano, 2012, 6, 6741-6750.	14.6	106
29	Large-Area Two-Dimensional Layered Hexagonal Boron Nitride Grown on Sapphire by Metalorganic Vapor Phase Epitaxy. Crystal Growth and Design, 2016, 16, 3409-3415.	3.0	106
30	Er3+-doped PbF2: Comparison between nanocrystals in glass-ceramics and bulk single crystals. Journal of Solid State Chemistry, 2006, 179, 1995-2003.	2.9	103
31	Nucleation Antibunching in Catalyst-Assisted Nanowire Growth. Physical Review Letters, 2010, 104, 135501.	7.8	100
32	Origin of light scattering in ytterbium doped calcium fluoride transparent ceramic for high power lasers. Journal of the European Ceramic Society, 2011, 31, 1619-1630.	5.7	98
33	Metal organic vapor phase epitaxy growth of GaAsN on GaAs using dimethylhydrazine and tertiarybutylarsine. Applied Physics Letters, 1997, 70, 2861-2863.	3.3	97
34	Subpicosecond pulse generation at 134GHz using a quantum-dash-based Fabry-Perot laser emitting at 1.56μm. Applied Physics Letters, 2006, 88, 241105.	3.3	93
35	Mechanistic Insight and Optimization of InP Nanocrystals Synthesized with Aminophosphines. Chemistry of Materials, 2016, 28, 5925-5934.	6.7	93
36	Evidence for Flat Bands near the Fermi Level in Epitaxial Rhombohedral Multilayer Graphene. ACS Nano, 2015, 9, 5432-5439.	14.6	92

#	Article	IF	CITATIONS
37	Incorporation and redistribution of impurities into silicon nanowires during metal-particle-assisted growth. Nature Communications, 2014, 5, 4134.	12.8	91
38	Role of nonlinear effects in nanowire growth and crystal phase. Physical Review B, 2009, 80, .	3.2	90
39	Dynamics of Colloids in Single Solid-State Nanopores. Journal of Physical Chemistry B, 2011, 115, 2890-2898.	2.6	86
40	Composition profiling of InAsâ^•GaAs quantum dots. Applied Physics Letters, 2004, 85, 3717-3719.	3.3	85
41	Selective CO ₂ methanation on Ru/TiO ₂ catalysts: unravelling the decisive role of the TiO ₂ support crystal structure. Catalysis Science and Technology, 2016, 6, 8117-8128.	4.1	84
42	Growth kinetics of a single <mml:math <br="" xmlns:mml="http://www.w3.org/1998/Math/MathML">display="inline"><mml:msub><mml:mtext>InP</mml:mtext><mml:mrow><mml:mn>1</mml:mn><ml:mo>â^`< Physical Review B, 2010, 81, .</ml:mo></mml:mrow></mml:msub></mml:math>	/m sce :mo>	<rsھl:mi>x<!--</td--></r
43	Synthesis of Zinc and Lead Chalcogenide Core and Core/Shell Nanoplatelets Using Sequential Cation Exchange Reactions. Chemistry of Materials, 2014, 26, 3002-3008.	6.7	83
44	Phase Selection in Self-catalyzed GaAs Nanowires. Nano Letters, 2020, 20, 1669-1675.	9.1	83
45	GalnAs/GaAs quantum-well growth assisted by Sb surfactant: Toward 1.3â€,μm emission. Applied Physics Letters, 2004, 84, 3981-3983.	3.3	81
46	Rare-earth doped oxyfluoride glass-ceramics and fluoride ceramics: Synthesis and optical properties. Optical Materials, 2007, 29, 1263-1270.	3.6	81
47	In situ generation of indium catalysts to grow crystalline silicon nanowires at low temperature on ITO. Journal of Materials Chemistry, 2008, 18, 5187.	6.7	81
48	Carbon Nanotube Translocation to Distant Organs after Pulmonary Exposure: Insights fromin Situ14C-Radiolabeling and Tissue Radioimaging. ACS Nano, 2014, 8, 5715-5724.	14.6	81
49	Structural and compositional characterization of MOVPE GaN thin films transferred from sapphire to glass substrates using chemical lift-off and room temperature direct wafer bonding and GaN wafer scale MOVPE growth on ZnO-buffered sapphire. Journal of Crystal Growth, 2013, 370, 63-67.	1.5	75
50	Effect of CeF3Addition on the Nucleation and Up-Conversion Luminescence in Transparent Oxyfluoride Glassâ~'Ceramics. Chemistry of Materials, 2005, 17, 2216-2222.	6.7	74
51	GaAs nanowires formed by Au-assisted molecular beam epitaxy: Effect of growth temperature. Journal of Crystal Growth, 2007, 301-302, 853-856.	1.5	73
52	Synthesis of silicon nanocrystals in silane plasmas for nanoelectronics and large area electronic devices. Journal Physics D: Applied Physics, 2007, 40, 2258-2266.	2.8	72
53	Structural properties of epitaxial SrTiO3 thin films grown by molecular beam epitaxy on Si(001). Journal of Applied Physics, 2006, 100, 124109.	2.5	67
54	Siliconâ€Microtube Scaffold Decorated with Anatase TiO ₂ as a Negative Electrode for a 3D Litiumâ€Ion Microbattery. Advanced Energy Materials, 2014, 4, 1301612.	19.5	67

#	Article	IF	CITATIONS
55	Wurtzite to Zinc Blende Phase Transition in GaAs Nanowires Induced by Epitaxial Burying. Nano Letters, 2008, 8, 1638-1643.	9.1	63
56	Magnetic properties and domain structure of (Ga,Mn)As films with perpendicular anisotropy. Physical Review B, 2006, 73, .	3.2	62
57	Atomically Sharp Interface in an h-BN-epitaxial graphene van der Waals Heterostructure. Scientific Reports, 2015, 5, 16465.	3.3	62
58	Structure of the GaAs/InP interface obtained by direct wafer bonding optimised for surface emitting optical devices. Journal of Applied Physics, 1997, 82, 4892-4903.	2.5	61
59	Electrolyte-Gated Field Effect Transistor to Probe the Surface Defects and Morphology in Films of Thick CdSe Colloidal Nanoplatelets. ACS Nano, 2014, 8, 3813-3820.	14.6	61
60	Novel Heterostructured Ge Nanowires Based on Polytype Transformation. Nano Letters, 2014, 14, 4828-4836.	9.1	61
61	Thermodynamic analysis of Zn-Cd-Te, Zn-Hg-Te and Cd-Hg-Te: phase separation in ZnxCd1â^'xTe and ZnxHg1â^'xTe. Journal of Crystal Growth, 1992, 117, 10-15.	1.5	60
62	Growth and optical characterizations of InAs quantum dots on InP substrate: towards a 1.55μm quantum dot laser. Journal of Crystal Growth, 2003, 251, 230-235.	1.5	60
63	Sharpening the Interfaces of Axial Heterostructures in Self-Catalyzed AlGaAs Nanowires: Experiment and Theory. Nano Letters, 2016, 16, 1917-1924.	9.1	60
64	Morphology of self-catalyzed GaN nanowires and chronology of their formation by molecular beam epitaxy. Nanotechnology, 2011, 22, 245606.	2.6	59
65	Quantum cascade lasers grown on silicon. Scientific Reports, 2018, 8, 7206.	3.3	56
66	Measuring and Modeling the Growth Dynamics of Self-Catalyzed GaP Nanowire Arrays. Nano Letters, 2018, 18, 701-708.	9.1	55
67	Focused ion beam sculpted membranes for nanoscience tooling. Microelectronic Engineering, 2006, 83, 1474-1477.	2.4	54
68	Type II heterostructures formed by zinc-blende inclusions in InP and GaAs wurtzite nanowires. Applied Physics Letters, 2010, 97, 041910.	3.3	54
69	Gas sensors boosted by two-dimensional h-BN enabled transfer on thin substrate foils: towards wearable and portable applications. Scientific Reports, 2017, 7, 15212.	3.3	54
70	Monolithic integration of InP based heterostructures on silicon using crystalline Gd2O3 buffers. Applied Physics Letters, 2007, 91, .	3.3	53
71	Zinc blende GaAsSb nanowires grown by molecular beam epitaxy. Nanotechnology, 2008, 19, 275605.	2.6	53
72	Multi-scale structuration of glasses: Observations of phase separation and nanoscale heterogeneities in glasses by Z-contrast scanning electron transmission microscopy. Journal of Non-Crystalline Solids, 2012, 358, 1257-1262.	3.1	53

#	Article	IF	CITATIONS
73	Strain in a silicon-on-insulator nanostructure revealed by 3D x-ray Bragg ptychography. Scientific Reports, 2015, 5, 9827.	3.3	52
74	Investigations on GaAsSbN/GaAs quantum wells for 1.3–1.55μm emission. Journal of Crystal Growth, 2001, 227-228, 553-557.	1.5	51
75	Monodispersed MOF-808 Nanocrystals Synthesized via a Scalable Room-Temperature Approach for Efficient Heterogeneous Peptide Bond Hydrolysis. Chemistry of Materials, 2021, 33, 7057-7066.	6.7	51
76	Anisotropic etching of InP with low sidewall and surface induced damage in inductively coupled plasma etching using SiCl4. Journal of Vacuum Science and Technology A: Vacuum, Surfaces and Films, 1997, 15, 626-632.	2.1	50
77	Investigations on GaInNAsSb quinary alloy for 1.5 μm laser emission on GaAs. Applied Physics Letters, 2003, 83, 1298-1300.	3.3	50
78	Nucleation efficiency of erbium and ytterbium fluorides in transparent oxyfluoride glass-ceramics. Journal of Materials Research, 2005, 20, 472-481.	2.6	50
79	Metamorphic approach to single quantum dot emission at 1.55î¼m on GaAs substrate. Journal of Applied Physics, 2008, 103, .	2.5	50
80	Morphology and composition of highly strained InGaAs and InGaAsN layers grown on GaAs substrate. Applied Physics Letters, 2004, 84, 203-205.	3.3	49
81	Determination of the Local Concentrations of Mn Interstitials and Antisite Defects inGaMnAs. Physical Review Letters, 2004, 93, 086107.	7.8	48
82	Fabrication and characterization of a room-temperature ZnO polariton laser. Applied Physics Letters, 2013, 102, .	3.3	48
83	Crystal growth of bullet-shaped magnetite in magnetotactic bacteria of the <i>Nitrospirae</i> phylum. Journal of the Royal Society Interface, 2015, 12, 20141288.	3.4	48
84	Transmission electron microscopy study of the InP/InGaAs and InGaAs/InP heterointerfaces grown by metalorganic vapor-phase epitaxy. Journal of Applied Physics, 2002, 92, 5749-5755.	2.5	47
85	Semibulk InGaN: A novel approach for thick, single phase, epitaxial InGaN layers grown by MOVPE. Journal of Crystal Growth, 2013, 370, 57-62.	1.5	47
86	Abrupt GaP/GaAs Interfaces in Self-Catalyzed Nanowires. Nano Letters, 2015, 15, 6036-6041.	9.1	47
87	Transmission electron microscopy observations of low-load indents in GaAs. Philosophical Magazine Letters, 1999, 79, 805-812.	1.2	46
88	Vapor-liquid-solid mechanisms: Challenges for nanosized quantum cluster/dot/wire materials. Journal of Applied Physics, 2006, 100, 044315.	2.5	46
89	Distributed Bragg reflectors based on diluted boron-based BAIN alloys for deep ultraviolet optoelectronic applications. Applied Physics Letters, 2012, 100, 051101.	3.3	44
90	Conductance Statistics from a Large Array of Sub-10 nm Molecular Junctions. ACS Nano, 2012, 6, 4639-4647.	14.6	44

6

#	Article	IF	CITATIONS
91	Boron distribution in the core of Si nanowire grown by chemical vapor deposition. Journal of Applied Physics, 2012, 111, 094909.	2.5	44
92	Uprooting defects to enable high-performance III–V optoelectronic devices on silicon. Nature Communications, 2019, 10, 4322.	12.8	44
93	Plastic deformation of Ill–V semiconductorsunder concentrated load. Progress in Crystal Growth and Characterization of Materials, 2003, 47, 1-43.	4.0	43
94	Hair Fiber as a Nanoreactor in Controlled Synthesis of Fluorescent Gold Nanoparticles. Nano Letters, 2012, 12, 6212-6217.	9.1	43
95	Universal description of III-V/Si epitaxial growth processes. Physical Review Materials, 2018, 2, .	2.4	43
96	Accommodation at the interface of highly dissimilar semiconductor/oxide epitaxial systems. Physical Review B, 2009, 80, .	3.2	42
97	Functionalized Solid-State Nanopore Integrated in a Reusable Microfluidic Device for a Better Stability and Nanoparticle Detection. ACS Applied Materials & Interfaces, 2017, 9, 41634-41640.	8.0	42
98	Reduced Lasing Thresholds in GeSn Microdisk Cavities with Defect Management of the Optically Active Region. ACS Photonics, 2020, 7, 2713-2722.	6.6	42
99	Structural characterisation of transparent oxyfluoride glass-ceramics. Journal of Materials Science, 2000, 35, 4849-4856.	3.7	41
100	Preparation and up-conversion luminescence of 8 nm rare-earth doped fluoride nanoparticles. Optics Express, 2008, 16, 14544.	3.4	41
101	Flexible metal-semiconductor-metal device prototype on wafer-scale thick boron nitride layers grown by MOVPE. Scientific Reports, 2017, 7, 786.	3.3	41
102	Mesoscopic scale description of nucleation processes in glasses. Applied Physics Letters, 2011, 99, .	3.3	40
103	Polarization dependence study of electroluminescence and absorption from InAsâ^•GaAs columnar quantum dots. Applied Physics Letters, 2007, 91, .	3.3	39
104	Wetâ€Route Synthesis and Characterization of Yb:CaF ₂ Optical Ceramics. Journal of the American Ceramic Society, 2016, 99, 1992-2000.	3.8	39
105	Structural and optical properties of low-density and In-rich InAsâ^•GaAs quantum dots. Journal of Applied Physics, 2007, 101, 024918.	2.5	38
106	Growth-in-place deployment of in-plane silicon nanowires. Applied Physics Letters, 2011, 99, .	3.3	38
107	Multilayered InGaN/GaN structure vs. single InGaN layer for solar cell applications: A comparative study. Acta Materialia, 2013, 61, 6587-6596.	7.9	38
108	Sidewall passivation assisted by a silicon coverplate during Cl2–H2 and HBr inductively coupled plasma etching of InP for photonic devices. Journal of Vacuum Science & Technology B, 2008, 26, 666-674.	1.3	37

#	Article	IF	CITATIONS
109	Photon Cascade from a Single Crystal Phase Nanowire Quantum Dot. Nano Letters, 2016, 16, 1081-1085.	9.1	37
110	Sidewall and surface induced damage comparison between reactive ion etching and inductive plasma etching of InP using a CH4/H2/O2 gas mixture. Journal of Vacuum Science and Technology A: Vacuum, Surfaces and Films, 1996, 14, 1056-1061.	2.1	36
111	Indentation-induced crystallization and phase transformation of amorphous germanium. Journal of Applied Physics, 2004, 96, 1464-1468.	2.5	36
112	Spontaneous compliance of the InPâ^•SrTiO3 heterointerface. Applied Physics Letters, 2008, 92, .	3.3	36
113	Elastic anisotropy of polycrystalline Au films: Modeling and respective contributions of X-ray diffraction, nanoindentation and Brillouin light scattering. Acta Materialia, 2010, 58, 4998-5008.	7.9	36
114	FIB carving of nanopores into suspended graphene films. Microelectronic Engineering, 2012, 97, 311-316.	2.4	36
115	Strain and composition of capped Ge/Si self-assembled quantum dots grown by chemical vapor deposition. Applied Physics Letters, 2000, 77, 370-372.	3.3	35
116	Comparison of light- and heavy-ion-irradiated quantum-wells for use as ultrafast saturable absorbers. Applied Physics Letters, 2001, 79, 2722-2724.	3.3	34
117	Composition-Dependent Interfacial Abruptness in Au-Catalyzed Si _{1–<i>x</i>} Ge _{<i>x</i>} /Si/Si _{1–<i>x</i>} Ge _{<i>x</i>} Nanowire Heterostructures. Nano Letters, 2014, 14, 5140-5147.	9.1	34
118	Metal–organic framework/graphene oxide composites for CO ₂ capture by microwave swing adsorption. Journal of Materials Chemistry A, 2021, 9, 13135-13142.	10.3	34
119	Low-damage dry-etched grating on an MQW active layer and dislocation-free InP regrowth for 1.55-/spl mu/m complex-coupled DFB lasers fabrication. IEEE Photonics Technology Letters, 1998, 10, 1070-1072.	2.5	33
120	Ultrafast saturable absorption at 1.55 μm in heavy-ion-irradiated quantum-well vertical cavity. Applied Physics Letters, 2000, 76, 1371-1373.	3.3	33
121	1.5â€[micro sign]m laser on GaAs with GalnNAsSb quinary quantum well. Electronics Letters, 2003, 39, 519.	1.0	33
122	InAsâ^•InP(001) quantum dots emitting at 1.55μm grown by low-pressure metalorganic vapor-phase epitaxy. Applied Physics Letters, 2005, 87, 253114.	3.3	33
123	Scanning tunneling spectroscopy of cleaved InAs/GaAs quantum dots at low temperatures. Physical Review B, 2008, 77, .	3.2	33
124	Direct FIB fabrication and integration of "single nanopore devices―for the manipulation of macromolecules. Microelectronic Engineering, 2010, 87, 1300-1303.	2.4	33
125	Direct growth of GaAs-based structures on exactly (001)-oriented Ge/Si virtual substrates: reduction of the structural defect density and observation of electroluminescence at room temperature under CW electrical injection. Journal of Crystal Growth, 2004, 265, 53-59.	1.5	32
126	Pseudomorphic molecular beam epitaxy growth of γ-Al2O3(001) on Si(001) and evidence for spontaneous lattice reorientation during epitaxy. Applied Physics Letters, 2006, 89, 232907.	3.3	32

#	Article	IF	CITATIONS
127	Highly crystalline urchin-like structures made of ultra-thin zinc oxide nanowires. RSC Advances, 2014, 4, 47234-47239.	3.6	32
128	Ultrathin PECVD epitaxial Si solar cells on glass via low-temperature transfer process. Progress in Photovoltaics: Research and Applications, 2016, 24, 1075-1084.	8.1	32
129	Coupled HgSe Colloidal Quantum Wells through a Tunable Barrier: A Strategy To Uncouple Optical and Transport Band Gap. Chemistry of Materials, 2018, 30, 4065-4072.	6.7	32
130	Effect of layer stacking and p-type doping on the performance of InAsâ^•InP quantum-dash-in-a-well lasers emitting at 1.55μm. Applied Physics Letters, 2006, 89, 241123.	3.3	31
131	Wetting layer states of InAsâ^•GaAs self-assembled quantum dot structures: Effect of intermixing and capping layer. Journal of Applied Physics, 2007, 101, 063539.	2.5	31
132	Large Array of Subâ€10â€nm Singleâ€Grain Au Nanodots for use in Nanotechnology. Small, 2011, 7, 2607-2613.	10.0	31
133	Deep structural analysis of novel BGaN material layers grown by MOVPE. Journal of Crystal Growth, 2011, 315, 288-291.	1.5	31
134	Structural and optical properties of nanodots, nanowires, and multi-quantum wells of III-nitride grown by MOVPE nano-selective area growth. Journal of Crystal Growth, 2011, 315, 160-163.	1.5	31
135	Growth of Vertical GaAs Nanowires on an Amorphous Substrate via a Fiber-Textured Si Platform. Nano Letters, 2013, 13, 2743-2747.	9.1	31
136	BAIN thin layers for deep UV applications. Physica Status Solidi (A) Applications and Materials Science, 2015, 212, 745-750.	1.8	31
137	Selective area heteroepitaxy of GaSb on GaAs (001) for in-plane InAs nanowire achievement. Nanotechnology, 2016, 27, 505301.	2.6	31
138	Atomic-plane-thick reconstruction across the interface during heteroepitaxial bonding of InP-clad quantum wells on silicon. Applied Physics Letters, 2013, 102, .	3.3	30
139	AlGaN-based MQWs grown on a thick relaxed AlGaN buffer on AlN templates emitting at 285 nm. Optical Materials Express, 2015, 5, 380.	3.0	30
140	Biomimetic Nanotubes Based on Cyclodextrins for Ion-Channel Applications. Nano Letters, 2015, 15, 7748-7754.	9.1	30
141	Oxide glass used as inorganic template for fluorescent fluoride nanoparticles synthesis. Optical Materials, 2006, 28, 1401-1404.	3.6	29
142	Submicron-diameter semiconductor pillar microcavities with very high quality factors. Applied Physics Letters, 2007, 90, 091120.	3.3	29
143	Metallic Functionalization of CdSe 2D Nanoplatelets and Its Impact on Electronic Transport. Journal of Physical Chemistry C, 2016, 120, 12351-12361.	3.1	29
144	Structural effects of the thermal treatment on a GalnNAs/GaAs superlattice. Applied Physics Letters, 2001, 79, 1795-1797.	3.3	28

#	Article	IF	CITATIONS
145	Thermal stability of ion-irradiated InGaAs with (sub-) picosecond carrier lifetime. Applied Physics Letters, 2003, 82, 856-858.	3.3	28
146	Influence of Ce3+ doping on the structure and luminescence of Er3+-doped transparent glass-ceramics. Optical Materials, 2006, 28, 638-642.	3.6	28
147	Growth and characterization of InAs columnar quantum dots on GaAs substrate. Journal of Applied Physics, 2007, 102, 033502.	2.5	28
148	Band offsets at zincblende-wurtzite GaAs nanowire sidewall surfaces. Applied Physics Letters, 2013, 103, .	3.3	28
149	New insights into the Mo/Cu(In,Ga)Se2 interface in thin film solar cells: Formation and properties of the MoSe2 interfacial layer. Journal of Chemical Physics, 2016, 145, 154702.	3.0	28
150	Low temperature plasma enhanced CVD epitaxial growth of silicon on GaAs: a new paradigm for III-V/Si integration. Scientific Reports, 2016, 6, 25674.	3.3	28
151	Shear-driven phase transformation in silicon nanowires. Nanotechnology, 2018, 29, 125601.	2.6	28
152	Band-Gap Landscape Engineering in Large-Scale 2D Semiconductor van der Waals Heterostructures. ACS Nano, 2021, 15, 7279-7289.	14.6	28
153	Structural characterisation of transparent oxyfluoride glass-ceramics. Journal of Materials Science, 2000, 35, 4849-4856.	3.7	27
154	Subpicosecond pulse generation at 134â€CHz and low radiofrequency spectral linewidth in quantum dash-based Fabry-Perot lasers emitting at 1.5â€[micro sign]m. Electronics Letters, 2006, 42, 91.	1.0	27
155	Metal organic vapor phase epitaxy of InAsP/InP(001) quantum dots for 1.55μm applications: Growth, structural, and optical properties. Journal of Applied Physics, 2008, 104, 043504.	2.5	27
156	Nanometer-scale, quantitative composition mappings of InGaN layers from a combination of scanning transmission electron microscopy and energy dispersive x-ray spectroscopy. Nanotechnology, 2012, 23, 455707.	2.6	27
157	Silicon surface preparation for III-V molecular beam epitaxy. Journal of Crystal Growth, 2015, 413, 17-24.	1.5	27
158	<i>In situ</i> passivation of GaAsP nanowires. Nanotechnology, 2017, 28, 495707.	2.6	27
159	Fast radiative quantum dots: From single to multiple photon emission. Applied Physics Letters, 2007, 90, 223118.	3.3	26
160	Synthesis and photoluminescence properties of silicon nanowires treated by high-pressure water vapor annealing. Physica Status Solidi (A) Applications and Materials Science, 2007, 204, 1302-1306.	1.8	26
161	A semiconductor laser device for the generation of surface-plasmons upon electrical injection. Optics Express, 2009, 17, 9391.	3.4	26
162	Encapsulation of Microperoxidase-8 in MIL-101(Cr)-X Nanoparticles: Influence of Metal–Organic Framework Functionalization on Enzymatic Immobilization and Catalytic Activity. ACS Applied Nano Materials, 2020, 3, 3233-3243.	5.0	26

#	Article	IF	CITATIONS
163	Degradation Mechanism of Porous Metal-Organic Frameworks by In Situ Atomic Force Microscopy. Nanomaterials, 2021, 11, 722.	4.1	26
164	Bimodal distribution of Indium composition in arrays of low-pressure metalorganic-vapor-phase-epitaxy grown InGaAs/GaAs quantum dots. Applied Physics Letters, 2001, 79, 2157-2159.	3.3	25
165	Silicon–on–insulator waveguide photodetector with Ge/Si self-assembled islands. Journal of Applied Physics, 2002, 92, 1858-1861.	2.5	25
166	Subsurface deformations induced by a Vickers indenter in GaAs/AlGaAs superlattice. Journal of Materials Science Letters, 2002, 21, 401-404.	0.5	25
167	Polarization dependence of electroluminescence from closely-stacked and columnar quantum dots. Optical and Quantum Electronics, 2008, 40, 239-248.	3.3	25
168	Characteristics of the surface microstructures in thick InGaN layers on GaN. Optical Materials Express, 2013, 3, 1111.	3.0	25
169	FIB patterning of dielectric, metallized and graphene membranes: A comparative study. Microelectronic Engineering, 2014, 121, 87-91.	2.4	25
170	Evidence for a narrow band gap phase in $1T\hat{a}\in^2$ WS2 nanosheet. Applied Physics Letters, 2019, 115, .	3.3	25
171	Electroluminescence from nanocrystals above 2 µm. Nature Photonics, 2022, 16, 38-44.	31.4	25
172	Nanoindentation of GaAs compliant substrates. Philosophical Magazine A: Physics of Condensed Matter, Structure, Defects and Mechanical Properties, 2000, 80, 2899-2911.	0.6	24
173	Anisotropic and Smooth Inductively Coupled Plasma Etching of III-V Laser Waveguides Using HBr-O[sub 2] Chemistry. Journal of the Electrochemical Society, 2008, 155, H778.	2.9	24
174	Surface-emitting quantum cascade lasers with metallic photonic-crystal resonators. Applied Physics Letters, 2009, 94, 221101.	3.3	24
175	Wurtzite InP/InAs/InP core–shell nanowires emitting at telecommunication wavelengths on Si substrate. Nanotechnology, 2011, 22, 405702.	2.6	24
176	Excitonic properties of wurtzite InP nanowires grown on silicon substrate. Nanotechnology, 2013, 24, 035704.	2.6	24
177	Multifunctional hybrid silica nanoparticles based on [Mo6Br14]2â^' phosphorescent nanosized clusters, magnetic l³-Fe2O3 and plasmonic gold nanoparticles. Journal of Colloid and Interface Science, 2014, 424, 132-140.	9.4	24
178	Wave-Function Engineering in HgSe/HgTe Colloidal Heterostructures To Enhance Mid-infrared Photoconductive Properties. Nano Letters, 2018, 18, 4590-4597.	9.1	24
179	Inhibition of thickness variations during growth of InAsP/InGaP and InAsP/InGaAsP multiquantum wells with high compensated strains. Applied Physics Letters, 1996, 69, 2279-2281.	3.3	23
180	1.3 μm strain-compensated InAsP/InGaP electroabsorption modulator structure grown by atmospheric pressure metal–organic vapor epitaxy. Applied Physics Letters, 1997, 70, 96-98.	3.3	23

#	Article	IF	CITATIONS
181	Ge/Si self-assembled quantum dots grown on Si(001) in an industrial high-pressure chemical vapor deposition reactor. Journal of Applied Physics, 1999, 86, 1145-1148.	2.5	23
182	Columnar quantum dashes for an active region in polarization independent semiconductor optical amplifiers at 1.5511/4m. Applied Physics Letters, 2008, 93, .	3.3	23
183	Growth-interruption-induced low-density InAs quantum dots on GaAs. Journal of Applied Physics, 2008, 104, .	2.5	23
184	Shape-engineered epitaxial InGaAs quantum rods for laser applications. Applied Physics Letters, 2008, 92, 121102.	3.3	23
185	Growth and structural characterization of GaAs/GaAsSb axial heterostructured nanowires. Journal of Crystal Growth, 2009, 311, 1847-1850.	1.5	23
186	GaP/GaAs1â^'xPx nanowires fabricated with modulated fluxes: A step towards the realization of superlattices in a single nanowire. Journal of Crystal Growth, 2011, 323, 293-296.	1.5	23
187	Growth temperature dependence of exciton lifetime in wurtzite InP nanowires grown on silicon substrates. Applied Physics Letters, 2012, 100, .	3.3	23
188	Investigation of a relaxation mechanism specific to InGaN for improved MOVPE growth of nitride solar cell materials. Physica Status Solidi (A) Applications and Materials Science, 2012, 209, 25-28.	1.8	23
189	Improving InGaN heterojunction solar cells efficiency using a semibulk absorber. Solar Energy Materials and Solar Cells, 2017, 159, 405-411.	6.2	23
190	Correlating Structure and Detection Properties in HgTe Nanocrystal Films. Nano Letters, 2021, 21, 4145-4151.	9.1	23
191	Zinc-blende group III-V/group IV epitaxy: Importance of the miscut. Physical Review Materials, 2020, 4, .	2.4	23
192	Synthesis of Fluoride Nanoparticles in Non-Aqueous Nanoreactors. Luminescence Study of Eu3+:CaF2. Zeitschrift Fur Anorganische Und Allgemeine Chemie, 2006, 632, 1538-1543.	1.2	22
193	Growth of crystalline γâ€Al2O3 on Si by molecular beam epitaxy: Influence of the substrate orientation. Journal of Applied Physics, 2007, 102, 024101.	2.5	22
194	Photoluminescence from a single InGaAs epitaxial quantum rod. Applied Physics Letters, 2008, 92, 021901.	3.3	22
195	Quasi one-dimensional transport in single GaAs/AlGaAs core-shell nanowires. Applied Physics Letters, 2011, 98, .	3.3	22
196	A Stressâ€Free and Textured GaP Template on Silicon for Solar Water Splitting. Advanced Functional Materials, 2018, 28, 1801585.	14.9	22
197	Development of reflective back contacts for high-efficiency ultrathin Cu(In,Ga)Se2 solar cells. Thin Solid Films, 2019, 672, 1-6.	1.8	22
198	Luminescence of polymorphous silicon carbon alloys. Optical Materials, 2005, 27, 953-957.	3.6	21

#	Article	IF	CITATIONS
199	Mid-infrared intersublevel absorption of vertically electronically coupled InAs quantum dots. Applied Physics Letters, 2005, 87, 173113.	3.3	21
200	Elastic behavior of polycrystalline thin films inferred from in situ micromechanical testing and modeling. Applied Physics Letters, 2006, 89, 061911.	3.3	21
201	Optics with single nanowires. Comptes Rendus Physique, 2008, 9, 804-815.	0.9	21
202	Pressure-Dependent Photoluminescence Study of Wurtzite InP Nanowires. Nano Letters, 2016, 16, 2926-2930.	9.1	21
203	Solid-State Nanopore Easy Chip Integration in a Cheap and Reusable Microfluidic Device for Ion Transport and Polymer Conformation Sensing. ACS Sensors, 2018, 3, 2129-2137.	7.8	21
204	Effect of the orientations and polarities of GaAs substrates CdTe buffer layer structural properties. Materials Science and Engineering B: Solid-State Materials for Advanced Technology, 1993, 16, 145-150.	3.5	20
205	Development of robust interfaces based on crystalline γ-Al2O3(001) for subsequent deposition of amorphous high-lº oxides. Microelectronic Engineering, 2007, 84, 2243-2246.	2.4	20
206	Nondestructive three-dimensional imaging of crystal strain and rotations in an extended bonded semiconductor heterostructure. Physical Review B, 2015, 92, .	3.2	20
207	Role of compositional fluctuations and their suppression on the strain and luminescence of InGaN alloys. Journal of Applied Physics, 2015, 117, 055705.	2.5	20
208	Dynamic Characterization of III-Nitride-Based High-Speed Photodiodes. IEEE Photonics Journal, 2017, 9, 1-7.	2.0	20
209	In-plane InSb nanowires grown by selective area molecular beam epitaxy on semi-insulating substrate. Nanotechnology, 2018, 29, 305705.	2.6	20
210	Polarization- and diffraction-controlled second-harmonic generation from semiconductor metasurfaces. Journal of the Optical Society of America B: Optical Physics, 2019, 36, E55.	2.1	20
211	All-optical discrimination at 1.5 [micro sign]m using an ultrafast saturable absorber vertical cavity device. Electronics Letters, 2000, 36, 1486.	1.0	19
212	Indentation-induced deformations of GaAs(011) at a high temperature. Philosophical Magazine, 2003, 83, 1653-1673.	1.6	19
213	Reactive-ion etching of high-Q and submicron-diameter GaAsâ^•AlAs micropillar cavities. Journal of Vacuum Science & Technology an Official Journal of the American Vacuum Society B, Microelectronics Processing and Phenomena, 2005, 23, 2499.	1.6	19
214	Low density of self-assembled InAs quantum dots grown by solid-source molecular beam epitaxy on InP(001). Applied Physics Letters, 2006, 89, 123112.	3.3	19
215	1.43â€[micro sign]m InAs bilayer quantum dot lasers on GaAs substrate. Electronics Letters, 2006, 42, 638.	1.0	19
216	Growth of InAs bilayer quantum dots for long-wavelength laser emission on GaAs. Journal of Crystal Growth. 2007. 301-302. 959-962.	1.5	19

#	Article	IF	CITATIONS
217	Smooth sidewall in InP-based photonic crystal membrane etched by N[sub 2]-based inductively coupled plasma. Journal of Vacuum Science & Technology B, 2008, 26, 1326.	1.3	19
218	Self-assembled Ge nanocrystals on BaTiO3â^•SrTiO3â^•Si(001). Applied Physics Letters, 2008, 92, .	3.3	19
219	Polarization Properties of Columnar Quantum Dots: Effects of Aspect Ratio and Compositional Contrast. IEEE Journal of Quantum Electronics, 2010, 46, 197-204.	1.9	19
220	Abrupt GaP/Si hetero-interface using bistepped Si buffer. Applied Physics Letters, 2015, 107, .	3.3	19
221	InAs quantum dot in a needlelike tapered InP nanowire: a telecom band single photon source monolithically grown on silicon. Nanoscale, 2019, 11, 21847-21855.	5.6	19
222	Engineering a Robust Flat Band in III–V Semiconductor Heterostructures. Nano Letters, 2021, 21, 680-685.	9.1	19
223	Polarity-induced changes in the nanoindentation response of GaAs. Journal of Materials Research, 2004, 19, 131-136.	2.6	18
224	Imaging the electric properties of InAsâ^•InP(001) quantum dots capped with a thin InP layer by conductive atomic force microscopy: Evidence of memory effect. Applied Physics Letters, 2006, 89, 112115.	3.3	18
225	Synthesis of long group IV semiconductor nanowires by molecular beam epitaxy. Nanoscale Research Letters, 2011, 6, 113.	5.7	18
226	Nanoscale selective area growth of thick, dense, uniform, In-rich, InGaN nanostructure arrays on GaN/sapphire template. Journal of Applied Physics, 2014, 116, .	2.5	18
227	Pushing Absorption of Perovskite Nanocrystals into the Infrared. Nano Letters, 2020, 20, 3999-4006.	9.1	18
228	Crystal Phase Control during Epitaxial Hybridization of IIIâ€V Semiconductors with Silicon. Advanced Electronic Materials, 2022, 8, 2100777.	5.1	18
229	GeSnOI mid-infrared laser technology. Light: Science and Applications, 2021, 10, 232.	16.6	18
230	Low-load deformation of InP under contact loading; comparison with GaAs. Philosophical Magazine A: Physics of Condensed Matter, Structure, Defects and Mechanical Properties, 2002, 82, 1953-1961.	0.6	17
231	Microphotoluminescence of exciton and biexciton around 1.5μm from a single InAsâ^•InP(001) quantum dot. Applied Physics Letters, 2006, 88, 133101.	3.3	17
232	Study of radial growth rate and size control of silicon nanocrystals in square-wave-modulated silane plasmas. Applied Physics Letters, 2007, 91, 111501.	3.3	17
233	Controlling the Aspect Ratio of Quantum Dots: From Columnar Dots to Quantum Rods. IEEE Journal of Selected Topics in Quantum Electronics, 2008, 14, 1204-1213.	2.9	17
234	Exploration of the ultimate patterning potential achievable with focused ion beams. Ultramicroscopy, 2009, 109, 457-462.	1.9	17

#	Article	IF	CITATIONS
235	InAs/InP nanowires grown by catalyst assisted molecular beam epitaxy on silicon substrates. Journal of Crystal Growth, 2012, 344, 45-50.	1.5	17
236	InP1â´'xAsx quantum dots in InP nanowires: A route for single photon emitters. Journal of Crystal Growth, 2013, 378, 519-523.	1.5	17
237	Fine-tuning of the interface in high-quality epitaxial silicon films deposited by plasma-enhanced chemical vapor deposition at 200 °C. Journal of Materials Research, 2013, 28, 1626-1632.	2.6	17
238	Single step fabrication of N-doped graphene/Si3N4/SiC heterostructures. Nano Research, 2014, 7, 835-843.	10.4	17
239	Selective target protein detection using a decorated nanopore into a microfluidic device. Biosensors and Bioelectronics, 2021, 183, 113195.	10.1	17
240	Deformations induced by a Vickers indentor in InP at room temperature. EPJ Applied Physics, 2000, 12, 31-36.	0.7	16
241	Devitrification of fluorozirconate glasses: from nucleation to spinodal decomposition. Journal of Non-Crystalline Solids, 2001, 284, 85-90.	3.1	16
242	Comparison of GalnNAs/GaAs and GalnNAs/GaNAs/GaAs quantum wells emitting over 1.3μm wavelength. Journal of Crystal Growth, 2003, 251, 403-407.	1.5	16
243	Characterization of piezoelectric and pyroelectric properties of MOVPE-grown strained (111)A InGaAs/GaAs QW structures by modulation spectroscopy. Physica Status Solidi A, 2003, 195, 260-264.	1.7	16
244	Indentation punching through thin (011) InP. Journal of Materials Science, 2004, 39, 943-949.	3.7	16
245	Structural and photoluminescence studies of InAsN quantum dots grown on GaAs by MBE. Journal of Crystal Growth, 2006, 290, 80-86.	1.5	16
246	InAs nanocrystals on SiO2â^•Si by molecular beam epitaxy for memory applications. Applied Physics Letters, 2007, 91, 133114.	3.3	16
247	GaN/AlN freeâ€standing nanowires grown by molecular beam epitaxy. Physica Status Solidi C: Current Topics in Solid State Physics, 2008, 5, 1556-1558.	0.8	16
248	Influence of the surface reconstruction on the growth of InP on SrTiO3(001). Journal of Crystal Growth, 2009, 311, 1042-1045.	1.5	16
249	Effect of Cl2- and HBr-based inductively coupled plasma etching on InP surface composition analyzed using <i>in situ</i> x-ray photoelectron spectroscopy. Journal of Vacuum Science and Technology A: Vacuum, Surfaces and Films, 2012, 30, .	2.1	16
250	Towards a monolithically integrated III–V laser on silicon: optimization of multi-quantum well growth on InP on Si. Semiconductor Science and Technology, 2013, 28, 094008.	2.0	16
251	Effect of arsenic on the optical properties of GaSb-based type II quantum wells with quaternary GaInAsSb layers. Journal of Applied Physics, 2013, 114, .	2.5	16
252	Quantitative evaluation of microtwins and antiphase defects in GaP/Si nanolayers for a III–V photonics platform on silicon using a laboratory X-ray diffraction setup. Journal of Applied Crystallography, 2015, 48, 702-710.	4.5	16

#	Article	IF	CITATIONS
253	Growth optimization and characterization of regular arrays of GaAs/AlGaAs core/shell nanowires for tandem solar cells on silicon. Nanotechnology, 2019, 30, 084005.	2.6	16
254	Up to 300â€K lasing with GeSn-On-Insulator microdisk resonators. Optics Express, 2022, 30, 3954.	3.4	16
255	TEM study of the morphological and compositional instabilities of InGaAsP epitaxial structures. Journal of Crystal Growth, 2000, 221, 12-19.	1.5	15
256	GaAs/GaAs twist-bonding for compliant substrates: interface structure and epitaxial growth. Applied Surface Science, 2000, 164, 15-21.	6.1	15
257	Origin of the bimodal distribution of low-pressure metal-organic-vapor-phase-epitaxy grown InGaAs/GaAs quantum dots. Journal of Applied Physics, 2002, 91, 3859-3863.	2.5	15
258	Metal-organic vapor-phase epitaxy of defect-free InGaAs/GaAs quantum dots emitting around 1.3μm. Journal of Crystal Growth, 2002, 235, 89-94.	1.5	15
259	Thermodynamical analysis of the shape and size dispersion ofInAsâ^•InP(001)quantum dots. Physical Review B, 2006, 73, .	3.2	15
260	Thermodynamic description of the competition between quantum dots and quantum dashes during metalorganic vapor phase epitaxy in theInAsâ^•InP(001)system: Experiment and theory. Physical Review B, 2006, 74, .	3.2	15
261	Directional growth of Ge on GaAs at 175°C using plasma-generated nanocrystals. Applied Physics Letters, 2008, 92, 103108.	3.3	15
262	High yield syntheses of reactive fluoride K1â^'x(Y,Ln)xF1+2x nanoparticles. Optical Materials, 2009, 31, 1177-1183.	3.6	15
263	Interface roughness transport in terahertz quantum cascade detectors. Applied Physics Letters, 2010, 96, 061111.	3.3	15
264	Multicharacterization approach for studying InAl(Ga)N/Al(Ga)N/GaN heterostructures for high electron mobility transistors. AIP Advances, 2014, 4, .	1.3	15
265	Nanoselective area growth and characterization of dislocation-free InGaN nanopyramids on AlN buffered Si(111) templates. Applied Physics Letters, 2015, 107, .	3.3	15
266	Microstructural and electrical investigation of Pd/Au ohmic contact on p-GaN. Journal of Vacuum Science and Technology B:Nanotechnology and Microelectronics, 2015, 33, 010603.	1.2	15
267	Nanoselective area growth of GaN by metalorganic vapor phase epitaxy on 4H-SiC using epitaxial graphene as a mask. Applied Physics Letters, 2016, 108, .	3.3	15
268	Characterization of antimonide based material grown by molecular epitaxy on vicinal silicon substrates via a low temperature AlSb nucleation layer. Journal of Crystal Growth, 2017, 477, 65-71.	1.5	15
269	Efficient incorporation and protection of lansoprazole in cyclodextrin metal-organic frameworks. International Journal of Pharmaceutics, 2020, 585, 119442.	5.2	15
270	Study of growth rate and composition variations in metalorganic vapour phase selective area epitaxy at atmospheric pressure and application to the growth of strained layer DBR lasers. Journal of Crystal Growth, 1997, 170, 639-644.	1.5	14

#	Article	IF	CITATIONS
271	Room-Temperature Plasticity of InAs. Physica Status Solidi A, 2000, 179, 153-158.	1.7	14
272	In-depth deformation of InP under a Vickers indentor. Journal of Materials Science, 2001, 36, 1343-1347.	3.7	14
273	Silicon-on-insulator and SiGe waveguide photodetectors with Ge/Si self-assembled islands. Physica E: Low-Dimensional Systems and Nanostructures, 2003, 16, 523-527.	2.7	14
274	Initial stage of the overgrowth of InP on InAsâ^•InP(001) quantum dots: Formation of InP terraces driven by preferential nucleation on quantum dot edges. Applied Physics Letters, 2006, 89, 031923.	3.3	14
275	Density of InAsâ^•InP(001) quantum dots grown by metal-organic vapor phase epitaxy: Independent effects of InAs and cap-layer growth rates. Applied Physics Letters, 2007, 91, .	3.3	14
276	TEM-nanoindentation studies of semiconducting structures. Micron, 2007, 38, 377-389.	2.2	14
277	Control of polarization and dipole moment in low-dimensional semiconductor nanostructures. Applied Physics Letters, 2009, 95, 221116.	3.3	14
278	Optically active defects in an InAsP/InP quantum well monolithically grown on SrTiO3(001). Applied Physics Letters, 2009, 95, .	3.3	14
279	Inductively coupled plasma etching of GaAs suspended photonic crystal cavities. Journal of Vacuum Science & Technology B, 2009, 27, 1909-1914.	1.3	14
280	Growth, structure and phase transitions of epitaxial nanowires of III-V semiconductors. Journal of Physics: Conference Series, 2010, 209, 012002.	0.4	14
281	Efficient photogeneration of charge carriers in silicon nanowires with a radial doping gradient. Nanotechnology, 2011, 22, 315710.	2.6	14
282	Design, Fabrication, and Characterization of Near-Milliwatt-Power RCLEDs Emitting at 390 nm. IEEE Photonics Journal, 2013, 5, 8400709-8400709.	2.0	14
283	Type I band alignment in GaAs81Sb19/GaAs core-shell nanowires. Applied Physics Letters, 2015, 107, .	3.3	14
284	Optical polarization properties of InAs/InP quantum dot and quantum rod nanowires. Nanotechnology, 2015, 26, 395701.	2.6	14
285	Low-loss orientation-patterned GaSb waveguides for mid-infrared parametric conversion. Optical Materials Express, 2017, 7, 3011.	3.0	14
286	Interface energy analysis of III–V islands on Si (001) in the Volmer-Weber growth mode. Applied Physics Letters, 2018, 113, .	3.3	14
287	Nanoscale electrical analyses of axial-junction GaAsP nanowires for solar cell applications. Nanotechnology, 2020, 31, 145708.	2.6	14
288	Control of the Mechanical Adhesion of III–V Materials Grown on Layered h-BN. ACS Applied Materials & Interfaces, 2020, 12, 55460-55466.	8.0	14

#	Article	IF	CITATIONS
289	Highly Ordered Boron Nitride/Epigraphene Epitaxial Films on Silicon Carbide by Lateral Epitaxial Deposition. ACS Nano, 2020, 14, 12962-12971.	14.6	14
290	Quantum well interband semiconductor lasers highly tolerant to dislocations. Optica, 2021, 8, 1397.	9.3	14
291	Ultrathin Ni nanowires embedded in <mml:math xmlns:mml="http://www.w3.org/1998/Math/MathML"><mml:msub><mml:mi>SrTiO</mml:mi><mml:mn>3: Vertical epitaxy, strain relaxation mechanisms, and solid-state amorphization. Physical Review Materials. 2018. 2</mml:mn></mml:msub></mml:math 	nl:mn> 2.4	ml:msub>
292	Effect of cap-layer growth rate on morphology and luminescence of InAsâ^InP(001) quantum dots grown by metal-organic vapor phase epitaxy. Journal of Applied Physics, 2006, 100, 033508.	2.5	13
293	Optical and electronic properties of GaAs-based structures with columnar quantum dots. Applied Physics Letters, 2007, 90, 181933.	3.3	13
294	Structure of nanoindentations in heavily n- and p-doped (001) GaAs. Acta Materialia, 2008, 56, 1417-1426.	7.9	13
295	Epitaxial growth of quantum rods with high aspect ratio and compositional contrast. Journal of Applied Physics, 2008, 104, .	2.5	13
296	Orientation dependent emission properties of columnar quantum dash laser structures. Applied Physics Letters, 2009, 94, 241113.	3.3	13
297	Time-resolved spectroscopy of InAsP/InP(001) quantum dots emitting near 2â€,μm. Applied Physics Letters, 2010, 97, 131907.	3.3	13
298	Evaluation of the surface bonding energy of an InP membrane bonded oxide-free to Si using instrumented nanoindentation. Applied Physics Letters, 2013, 103, 081901.	3.3	13
299	Random stacking sequences in III-V nanowires are correlated. Physical Review B, 2014, 89, .	3.2	13
300	Dual light-emitting nanoparticles: second harmonic generation combined with rare-earth photoluminescence. Journal of Materials Chemistry C, 2014, 2, 7681-7686.	5.5	13
301	High performance TiN gate contact on AlGaN/GaN transistor using a mechanically strain induced P-doping. Applied Physics Letters, 2014, 104, .	3.3	13
302	Threading dislocation free GaSb nanotemplates grown by selective molecular beam epitaxy on GaAs (001) for in-plane InAs nanowire integration. Journal of Crystal Growth, 2017, 477, 45-49.	1.5	13
303	GaAs (1 1 1) epilayers grown by MBE on Ge (1 1 1): Twin reduction and polarity. Journal of Crystal Growth, 2019, 519, 84-90.	1.5	13
304	Selective area molecular beam epitaxy of InSb nanostructures on mismatched substrates. Journal of Crystal Growth, 2019, 512, 6-10.	1.5	13
305	Submilliwatt optical bistability in wafer fused vertical cavity at 1.55-μm wavelength. IEEE Photonics Technology Letters, 1996, 8, 539-541.	2.5	12
306	Twist-bonded compliant substrates for III–V semiconductors heteroepitaxy. Applied Surface Science, 2001, 178, 134-139.	6.1	12

#	Article	IF	CITATIONS
307	Absolute determination of the asymmetry of the in-plane deformation of GaAs (001). Journal of Applied Physics, 2004, 95, 3984-3987.	2.5	12
308	Surface-plasmon distributed-feedback mid-infrared quantum cascade lasers based on hybrid plasmon/air-guided modes. Electronics Letters, 2008, 44, 807.	1.0	12
309	Epitaxial growth of silicon and germanium on (100)-oriented crystalline substrates by RF PECVD at 175 °C. EPJ Photovoltaics, 2012, 3, 30303.	1.6	12
310	Suppression of crack generation in AlGaN/GaN distributed Bragg reflectors grown by MOVPE. Journal of Crystal Growth, 2013, 370, 12-15.	1.5	12
311	Towards InAs/InGaAs/GaAs Quantum Dot Solar Cells Directly Grown on Si Substrate. Materials, 2015, 8, 4544-4552.	2.9	12
312	GaSb-based composite quantum wells for laser diodes operating in the telecom wavelength range near 1.55- <i>μ</i> m. Applied Physics Letters, 2015, 106, .	3.3	12
313	Largeâ€Area van der Waals Epitaxial Growth of Vertical IIIâ€Nitride Nanodevice Structures on Layered Boron Nitride. Advanced Materials Interfaces, 2019, 6, 1900207.	3.7	12
314	Effectiveness of selective area growth using van der Waals h-BN layer for crack-free transfer of large-size III-N devices onto arbitrary substrates. Scientific Reports, 2020, 10, 21709.	3.3	12
315	Single crystalline boron rich B(Al)N alloys grown by MOVPE. Applied Physics Letters, 2020, 116, .	3.3	12
316	Influence of Sapphire Substrate Orientation on the van der Waals Epitaxy of III-Nitrides on 2D Hexagonal Boron Nitride: Implication for Optoelectronic Devices. ACS Applied Nano Materials, 2022, 5, 791-800.	5.0	12
317	Evidence for highly p-type doping and type II band alignment in large scale monolayer WSe ₂ /Se-terminated GaAs heterojunction grown by molecular beam epitaxy. Nanoscale, 2022, 14, 5859-5868.	5.6	12
318	Non-linear solid solution strengthening of InGaAs alloy. Journal of Materials Science Letters, 2001, 20, 43-45.	0.5	11
319	Solid-solution strengthening in ordered InxGa1 â^ xP alloys. Philosophical Magazine Letters, 2004, 84, 373-381.	1.2	11
320	Structural studies of nano/micrometric semiconducting GalnP wires grown by MOCVD. Journal of Crystal Growth, 2004, 272, 198-203.	1.5	11
321	Mechanical response of wall-patterned GaAs surface. Acta Materialia, 2005, 53, 1907-1912.	7.9	11
322	Influence of deposition parameters and post-deposition plasma treatments on the photoluminescence of polymorphous silicon carbon alloys. Journal of Non-Crystalline Solids, 2006, 352, 1357-1360.	3.1	11
323	Time-multiplexed, inductively coupled plasma process with separate SiCl4 and O2 steps for etching of GaAs with high selectivity. Journal of Vacuum Science & Technology B, 2009, 27, 2270-2279.	1.3	11
324	Si Incorporation in InP Nanowires Grown by Au-Assisted Molecular Beam Epitaxy. Journal of Nanomaterials, 2009, 2009, 1-7.	2.7	11

#	Article	IF	CITATIONS
325	Effect of diffusion from a lateral surface on the rate of GaN nanowire growth. Semiconductors, 2012, 46, 838-841.	0.5	11
326	Effect of postgrowth heat treatment on the structural and optical properties of InP/InAsP/InP nanowires. Semiconductors, 2012, 46, 175-178.	0.5	11
327	Versatile cyclodextrin nanotube synthesis with functional anchors for efficient ion channel formation: design, characterization and ion conductance. Nanoscale, 2018, 10, 15303-15316.	5.6	11
328	Impact of the sequence of precursor introduction on the growth and properties of atomic layer deposited Al-doped ZnO films. Journal of Vacuum Science and Technology A: Vacuum, Surfaces and Films, 2018, 36, .	2.1	11
329	Wafer-scale MOVPE growth and characterization of highly ordered h-BN on patterned sapphire substrates. Journal of Crystal Growth, 2019, 509, 40-43.	1.5	11
330	Crystal phase engineering of self-catalyzed GaAs nanowires using a RHEED diagram. Nanoscale Advances, 2020, 2, 2127-2134.	4.6	11
331	Spray-Drying Polymer Encapsulation of CsPbBr3 Perovskite Nanocrystals with Enhanced Photostability for LED Downconverters. ACS Applied Nano Materials, 2021, 4, 7502-7512.	5.0	11
332	Imperfections in II–VI semiconductor layers epitaxially grown by organometallic chemical vapour deposition on GaAs. Journal of Crystal Growth, 1993, 129, 375-384.	1.5	10
333	Deformations of (011) GaAs under concentrated load. Journal of Materials Science Letters, 2001, 20, 1361-1364.	0.5	10
334	Control of nitrogen incorporation in Ga(In)NAs grown by metalorganic vapor phase epitaxy. Journal of Applied Physics, 2003, 94, 2752-2754.	2.5	10
335	Vickers indentation of thin GaAs (001) samples. Philosophical Magazine, 2004, 84, 3281-3298.	1.6	10
336	Telecom-wavelength single-photon sources for quantum communications. Journal of Physics Condensed Matter, 2007, 19, 225005.	1.8	10
337	Crystal orientation of GaAs islands grown on SrTiO3 (001) by molecular beam epitaxy. Applied Physics Letters, 2009, 95, 011907.	3.3	10
338	Surface-plasmon distributed-feedback quantum cascade lasers operating pulsed, room temperature. Applied Physics Letters, 2009, 95, 091105.	3.3	10
339	Nanoscale investigation of a radial p–n junction in self-catalyzed GaAs nanowires grown on Si (111). Nanoscale, 2018, 10, 20207-20217.	5.6	10
340	Guided-Mode Resonator Coupled with Nanocrystal Intraband Absorption. ACS Photonics, 2022, 9, 985-993.	6.6	10
341	Material Flow at the Surface of Indented Indium Phosphide. Physica Status Solidi A, 1997, 161, 415-427.	1.7	9
342	Step-bunching instability in strained-layer superlattices grown on vicinal substrates. Applied Physics Letters, 2000, 76, 306-308.	3.3	9

#	Article	IF	CITATIONS
343	Microscopic structure and optical properties of GaAs1â^'xNx/GaAs(001) interface grown by metalorganic vapor phase epitaxy. Applied Physics Letters, 2002, 80, 2460-2462.	3.3	9
344	Neutral and charged multi-exciton complexes in single InAs quantum dots grown on InP(001). Nanotechnology, 2006, 17, 1831-1834.	2.6	9
345	One-step nano-selective area growth (nano-SAG) of localized InAs/InP quantum dots: First step towards single-photon source applications. Journal of Crystal Growth, 2008, 310, 3413-3415.	1.5	9
346	Twin formation during the growth of InP on SrTiO3. Applied Physics Letters, 2009, 94, 231902.	3.3	9
347	Gold anchoring on Si sawtooth faceted nanowires. Europhysics Letters, 2011, 95, 18004.	2.0	9
348	Faceting mechanisms of Si nanowires and gold spreading. Journal of Materials Science, 2012, 47, 1609-1613.	3.7	9
349	Interface Intermixing in Type II InAs/GaInAsSb Quantum Wells Designed for Active Regions of Mid-Infrared-Emitting Interband Cascade Lasers. Nanoscale Research Letters, 2015, 10, 471.	5.7	9
350	Nonstoichiometric Low-Temperature Grown GaAs Nanowires. Nano Letters, 2015, 15, 6440-6445.	9.1	9
351	MOVPE of GaN-based mixed dimensional heterostructures on wafer-scale layered 2D hexagonal boron nitride—A key enabler of III-nitride flexible optoelectronics. APL Materials, 2021, 9, .	5.1	9
352	Misfit accommodation and dislocations in heteroepitaxial semiconductor layers: II-VI compounds on GaAs. Journal De Physique III, 1993, 3, 1189-1199.	0.3	9
353	Controlled steam oxidation of AlInAs for microelectronics and optoelectronics applications. Journal of Electronic Materials, 1997, 26, L32-L35.	2.2	8
354	Effects of annealing on structure of GaAs(001) nanoindentations. Philosophical Magazine Letters, 2003, 83, 149-158.	1.2	8
355	Elastic properties of polycrystalline gold thin films: Simulation and X-ray diffraction experiments. Surface and Coatings Technology, 2006, 201, 4300-4304.	4.8	8
356	Growth of vertical and defect free InP nanowires on SrTiO3(001) substrate and comparison with growth on silicon. Journal of Crystal Growth, 2012, 343, 101-104.	1.5	8
357	Influence of catalyst droplet diameter on the growth direction of InP nanowires grown on Si(001) substrate. Applied Physics Letters, 2013, 102, 243113.	3.3	8
358	Surface plasmon modulation induced by a direct-current electric field into gallium nitride thin film grown on Si(111) substrate. Applied Physics Letters, 2013, 102, 021905.	3.3	8
359	Void-free direct bonding of InP to Si: Advantages of low H-content and ozone activation. Journal of Vacuum Science and Technology B:Nanotechnology and Microelectronics, 2014, 32, 021201.	1.2	8
360	ZnS anisotropic nanocrystals using a one-pot low temperature synthesis. New Journal of Chemistry, 2015, 39, 90-93.	2.8	8

#	Article	IF	CITATIONS
361	Role of V-pits in the performance improvement of InGaN solar cells. Applied Physics Letters, 2016, 109, .	3.3	8
362	Morphology and valence band offset of GaSb quantum dots grown on GaP(001) and their evolution upon capping. Nanotechnology, 2017, 28, 225601.	2.6	8
363	Biomimetic ion channels formation by emulsion based on chemically modified cyclodextrin nanotubes. Faraday Discussions, 2018, 210, 41-54.	3.2	8
364	Physical mechanisms involved in the formation and operation of memory devices based on a monolayer of gold nanoparticle-polythiophene hybrid materials. Nanoscale Advances, 2019, 1, 2718-2726.	4.6	8
365	MOVPE van der Waals epitaxial growth of AlGaN/AlGaN multiple quantum well structures with deep UV emission on large scale 2D h-BN buffered sapphire substrates. Journal of Crystal Growth, 2019, 507, 352-356.	1.5	8
366	Interdiffusion of Al and Ga in AlN/AlGaN superlattices grown by ammonia-assisted molecular beam epitaxy. Superlattices and Microstructures, 2021, 150, 106801.	3.1	8
367	Monolithic Free-Standing Large-Area Vertical III-N Light-Emitting Diode Arrays by One-Step h-BN-Based Thermomechanical Self-Lift-Off and Transfer. ACS Applied Electronic Materials, 2021, 3, 2614-2621.	4.3	8
368	Electromodulation of the interband and intraband absorption of Ge/Si self-assembled islands. Physica E: Low-Dimensional Systems and Nanostructures, 2003, 16, 450-454.	2.7	7
369	Epitaxial growth of high-l [®] oxides on silicon. Thin Solid Films, 2008, 517, 197-200.	1.8	7
370	Confined VLS growth and structural characterization of silicon nanoribbons. Microelectronic Engineering, 2010, 87, 1522-1526.	2.4	7
371	Comparative optical studies of InGaAs/GaAs quantum wells grown by MBE on (100) and (311)A GaAs planes. Physica Status Solidi C: Current Topics in Solid State Physics, 2012, 9, 1621-1623.	0.8	7
372	Polarization properties of single and ensembles of InAs/InP quantum rod nanowires emitting in the telecom wavelengths. Journal of Applied Physics, 2013, 113, 193101.	2.5	7
373	Piezoelectric effect in InAs/InP quantum rod nanowires grown on silicon substrate. Applied Physics Letters, 2014, 104, 183101.	3.3	7
374	High quality thick InGaN nanostructures grown by nanoselective area growth for new generation photovoltaic devices. Physica Status Solidi (A) Applications and Materials Science, 2015, 212, 740-744.	1.8	7
375	Nanoscale elemental quantification in heterostructured SiGe nanowires. Nanoscale, 2015, 7, 8544-8553.	5.6	7
376	Synthesis of In0.1Ga0.9N/GaN structures grown by MOCVD and MBE for high speed optoelectronics. MRS Advances, 2016, 1, 1735-1742.	0.9	7
377	Lazarevicite-type short-range ordering in ternary III-V nanowires. Physical Review B, 2016, 94, .	3.2	7
378	In Situ Optical Monitoring of New Pathways in the Metal-Induced Crystallization of Amorphous Ge. Crystal Growth and Design, 2017, 17, 5783-5789.	3.0	7

#	Article	IF	CITATIONS
379	Electronic properties of (Sb;Bi)2Te3 colloidal heterostructured nanoplates down to the single particle level. Scientific Reports, 2017, 7, 9647.	3.3	7
380	Emission wavelength red-shift by using "semi-bulk―InGaN buffer layer in InGaN/InGaN multiple-quantum-well. Superlattices and Microstructures, 2017, 112, 279-286.	3.1	7
381	Study of the nucleation and growth of InP nanowires on silicon with gold-indium catalyst. Journal of Crystal Growth, 2017, 458, 96-102.	1.5	7
382	Correlated optical and structural analyses of individual GaAsP/GaP core–shell nanowires. Nanotechnology, 2019, 30, 304001.	2.6	7
383	Trap-Free Heterostructure of PbS Nanoplatelets on InP(001) by Chemical Epitaxy. ACS Nano, 2019, 13, 1961-1967.	14.6	7
384	Topological surface states in epitaxial <mml:math< td=""><td></td><td></td></mml:math<>		

#	Article	IF	CITATIONS
397	Interfacial abruptness in axial Si/SiGe heterostructures in nanowires probed by scanning capacitance microscopy. Physica Status Solidi (A) Applications and Materials Science, 2014, 211, 509-513.	1.8	6
398	Interplay between tightly focused excitation and ballistic propagation of polariton condensates in a ZnO microcavity. Physical Review B, 2015, 92, .	3.2	6
399	Structural and optical investigations of AlGaN MQWs grown on a relaxed AlGaN buffer on AlN templates for emission at 280nm. Journal of Crystal Growth, 2015, 432, 37-44.	1.5	6
400	High reflectance dielectric distributed Bragg reflectors for near ultra-violet planar microcavities: SiO2/HfO2 versus SiO2/SiNx. Journal of Applied Physics, 2016, 120, .	2.5	6
401	Sub-nanometrically resolved chemical mappings of quantum-cascade laser active regions. Semiconductor Science and Technology, 2016, 31, 055017.	2.0	6
402	An ultra-thin SiO2 ALD layer for void-free bonding of Ill–V material on silicon. Microelectronic Engineering, 2016, 162, 40-44.	2.4	6
403	Molecular-beam epitaxy of GaSb on 6°-offcut (0â€⁻0â€⁻1) Si using a GaAs nucleation layer. Journal of Crystal Growth, 2020, 529, 125299.	1.5	6
404	Stable and high yield growth of GaP and In _{0.2} Ga _{0.8} As nanowire arrays using In as a catalyst. Nanoscale, 2020, 12, 18240-18248.	5.6	6
405	Dynamics of Droplet Consumption in Vapor–Liquid–Solid III–V Nanowire Growth. Crystal Growth and Design, 2021, 21, 4647-4655.	3.0	6
406	3.3 Âμm interband-cascade resonant-cavity light-emitting diode with narrow spectral emission linewidth. Semiconductor Science and Technology, 2020, 35, 125029.	2.0	6
407	High-quality InAs/GaAs quantum dots grown by low-pressure metalorganic vapor-phase epitaxy. Journal of Crystal Growth, 1998, 195, 524-529.	1.5	5
408	Influence of the thermal treatment on the optical and structural properties of 1.3 μm emitting LP-MOVPE grown InAs/GaAs quantum dots. Optical Materials, 2001, 17, 263-266.	3.6	5
409	Low-load deformation of InP under contact loading; comparison with GaAs. Philosophical Magazine A: Physics of Condensed Matter, Structure, Defects and Mechanical Properties, 2002, 82, 1953-1961.	0.6	5
410	N-enrichment at the GaAs1â^'xNx/GaAs(001) interface: microstructure and optical properties. Journal of Crystal Growth, 2003, 248, 441-445.	1.5	5
411	Effects of GaNAsSb intermediate barriers on GaInNAsSb quantum well grown by molecular beam epitaxy. Journal of Crystal Growth, 2004, 263, 58-62.	1.5	5
412	TEM study of the indentation behaviour of thin Au film on GaAs. Thin Solid Films, 2004, 460, 150-155.	1.8	5
413	Growth of nanometric CuGaxOystructures on copper substrates. Nanotechnology, 2005, 16, 2790-2793.	2.6	5
414	Polarity influence on the indentation punching of thin {111} GaAs foils at elevated temperatures. Journal Physics D: Applied Physics, 2005, 38, 1140-1147.	2.8	5

#	Article	IF	CITATIONS
415	Optical and structural investigation of In1â^'xGaxP free-standing microrods. Journal of Applied Physics, 2005, 98, 053506.	2.5	5
416	GaNAsSb Alloy and Its Potential for Device Applications. , 2005, , 471-493.		5
417	InAs(Sb) quantum dots grown on GaAs by MBE. Physica Status Solidi C: Current Topics in Solid State Physics, 2006, 3, 3997-4000.	0.8	5
418	Cavity QED with a single QD inside an optical microcavity. Physica Status Solidi (B): Basic Research, 2006, 243, 3879-3884.	1.5	5
419	High-aspect-ratio inductively coupled plasma etching of InP using SiH4/Cl2: Avoiding the effect of electrode coverplate material. Journal of Vacuum Science and Technology B:Nanotechnology and Microelectronics, 2011, 29, 020601.	1.2	5
420	Atomic-plane-thick reconstruction across the interface during heteroepitaxial bonding of InP-clad quantum wells to Si. , 2012, , .		5
421	Gold nanocluster distribution on faceted and kinked Si nanowires. Thin Solid Films, 2012, 520, 3304-3308.	1.8	5
422	Characteristics of HgS nanoparticles formed in hair by a chemical reaction. Philosophical Magazine, 2013, 93, 137-151.	1.6	5
423	Structural and photoluminescence studies of highly crystalline un-annealed ZnO nanorods arrays synthesized by hydrothermal technique. Journal of Luminescence, 2013, 144, 234-240.	3.1	5
424	Comparison of chemical and laser lift-off for the transfer of InGaN-based p-i-n junctions from sapphire to glass substrates. , 2013, , .		5
425	Catalyst faceting during graphene layer crystallization in the course of carbon nanofiber growth. Carbon, 2014, 79, 93-102.	10.3	5
426	Oxide-Free Bonding of III-V-Based Material on Silicon and Nano-Structuration of the Hybrid Waveguide for Advanced Optical Functions. Photonics, 2015, 2, 1054-1064.	2.0	5
427	Crystallization of Si Templates of Controlled Shape, Size, and Orientation: Toward Micro- and Nanosubstrates. Crystal Growth and Design, 2015, 15, 2102-2109.	3.0	5
428	Importance of point defect reactions for the atomic-scale roughness of Ill–V nanowire sidewalls. Nanotechnology, 2019, 30, 324002.	2.6	5
429	Strain, magnetic anisotropy, and composition modulation in hybrid metal–oxide vertically assembled nanocomposites. MRS Bulletin, 2021, 46, 136-141.	3.5	5
430	A porous Ge/Si interface layer for defect-free III-V multi-junction solar cells on silicon. , 2019, , .		5
431	In‣itu Transmission Electron Microscopy Observation of Germanium Growth on Freestanding Graphene: Unfolding Mechanism of 3D Crystal Growth During Van der Waals Epitaxy. Small, 2022, 18, e2101890.	10.0	5
432	Regulated Dynamics with Two Monolayer Steps in Vapor–Solid–Solid Growth of Nanowires. ACS Nano, 2022, 16, 4397-4407.	14.6	5

#	Article	IF	CITATIONS
433	Base metallization stability in InP/InGaAs heterojunction bipolar transistors and its influence on leakage currents. Journal of Vacuum Science & Technology an Official Journal of the American Vacuum Society B, Microelectronics Processing and Phenomena, 1997, 15, 854.	1.6	4
434	Planar selective regrowth of high resistivity semi-insulating InP(Fe) by LP-MOVPE for buried lasers using TBP. Journal of Crystal Growth, 1998, 195, 479-484.	1.5	4
435	Plastic behaviour of an AlAs/GaAs superlattice with a short period. Philosophical Magazine Letters, 2001, 81, 223-231.	1.2	4
436	Plasticity of misoriented (001) GaAs surface. Journal of Materials Science Letters, 2003, 22, 565-567.	0.5	4
437	Structural properties of strained piezoelectric [111]A-oriented InGaAs/GaAs quantum well structures grown by MOVPE. Journal of Crystal Growth, 2003, 248, 359-363.	1.5	4
438	Further insight into the growth temperature influence of 1.3 μm GaInNAs/GaAs QWs on their properties. IEE Proceedings: Optoelectronics, 2004, 151, 279-283.	0.8	4
439	GSMBE growth of GalnAsP/InP 1.3μm-TM-lasers for monolithic integration with optical waveguide isolator. Journal of Crystal Growth, 2005, 278, 709-713.	1.5	4
440	Dislocation networks adapted to order the growth of III-V semiconductor nanostructures. Physica Status Solidi C: Current Topics in Solid State Physics, 2005, 2, 1933-1937.	0.8	4
441	Indentation deformation of thin {111} GaAs and InSb foils: influence of polarity. Philosophical Magazine Letters, 2005, 85, 1-12.	1.2	4
442	Nanoindentation response of a single micrometer-sized GaAs wall. Applied Physics Letters, 2005, 86, 163107.	3.3	4
443	Nanoindentation response of compound semiconductors. Physica Status Solidi C: Current Topics in Solid State Physics, 2007, 4, 3002-3009.	0.8	4
444	Modulated reflectivity probing of quantum dot and wetting layer states in InAs/GalnAsP/InP quantum dot laser structures. Physica Status Solidi (A) Applications and Materials Science, 2007, 204, 496-499.	1.8	4
445	Competition between InP and In2O3 islands during the growth of InP on SrTiO3. Journal of Applied Physics, 2008, 104, 033509.	2.5	4
446	Potential of semiconductor nanowires for single photon sources. Proceedings of SPIE, 2009, , .	0.8	4
447	InGaAs Quantum Dots Grown by Molecular Beam Epitaxy for Light Emission on Si Substrates. Journal of Nanoscience and Nanotechnology, 2011, 11, 9153-9159.	0.9	4
448	Composition and local strain mapping in Au-catalyzed axial Si/Ge nanowires. Nanotechnology, 2012, 23, 395701.	2.6	4
449	Heteroepitaxial bonding of Si for hybrid photonic devices. Materials Research Society Symposia Proceedings, 2013, 1510, 1.	0.1	4
450	Control of the interfacial abruptness of Au-catalyzed Si-Si1â^'xGex heterostructured nanowires grown by vapor–liquid–solid. Journal of Vacuum Science and Technology A: Vacuum, Surfaces and Films, 2014, 32, .	2.1	4

#	Article	IF	CITATIONS
451	Single-crystal nanopyramidal BGaN by nanoselective area growth on AlN/Si(111) and GaN templates. Nanotechnology, 2016, 27, 115602.	2.6	4
452	Nondestructive Characterization of Residual Threading Dislocation Density in HgCdTe Layers Grown on CdZnTe by Liquid-Phase Epitaxy. Journal of Electronic Materials, 2016, 45, 4518-4523.	2.2	4
453	Mask effect in nano-selective- area-growth by MOCVD on thickness enhancement, indium incorporation, and emission of InGaN nanostructures on AlN-buffered Si(111) substrates. Optical Materials Express, 2017, 7, 376.	3.0	4
454	Determination of the spin orbit coupling and crystal field splitting in wurtzite InP by polarization resolved photoluminescence. Applied Physics Letters, 2018, 112, .	3.3	4
455	Evidence and control of unintentional As-rich shells in GaAs _{1–<i>x</i>} P <i> _x </i> nanowires. Nanotechnology, 2019, 30, 294003.	2.6	4
456	Why is it difficult to grow spontaneous ZnO nanowires using molecular beam epitaxy?. Nanotechnology, 2020, 31, 385601.	2.6	4
457	Development of Micron Sized Photonic Devices Based on Deep GaN Etching. Photonics, 2021, 8, 68.	2.0	4
458	Electronic band gap of van der Waals Î \pm -As2Te3 crystals. Applied Physics Letters, 2021, 119, .	3.3	4
459	Density-controlled growth of vertical InP nanowires on Si(111) substrates. Nanotechnology, 2020, 31, 354003.	2.6	4
460	Phase separation and surface segregation in Co–Au–SrTiO3 thin films: Self-assembly of bilayered epitaxial nanocolumnar composites. Physical Review Materials, 2019, 3, .	2.4	4
461	Interphases and mechanical properties in carbon fibres/Al matrix composites. European Physical Journal Special Topics, 1993, 03, C7-1693-C7-1698.	0.2	3
462	Transmission electron microscope observations of dislocations in heteroepitaxial layers of CdTe-(CdHg)Te on GaAs. Materials Science and Engineering B: Solid-State Materials for Advanced Technology, 1997, 45, 76-84.	3.5	3
463	Long-range ordering of Ill–V semiconductor nanostructures by shallowly buried dislocation networks. Journal of Physics Condensed Matter, 2004, 16, 7941-7946.	1.8	3
464	Photoluminescence probing of non-radiative channels in hydrogenated In(Ga)As/GaAs quantum dots. Journal of Crystal Growth, 2004, 264, 334-338.	1.5	3
465	Stress-driven self-ordering of Ill–V nanostructures. Journal of Crystal Growth, 2005, 275, e2245-e2249.	1.5	3
466	Local electronic transport through InAs/InP(O O 1) quantum dots capped with a thin InP layer studied by an AFM conductive probe. Semiconductor Science and Technology, 2007, 22, 755-762.	2.0	3
467	Thermodynamic analysis of the shape, anisotropy and formation process of InAs/InP(001) quantum dots and quantum sticks grown by metalorganic vapor phase epitaxy. Surface Science, 2007, 601, 2765-2768.	1.9	3
468	De-relaxation of plastically relaxed InAs/GaAs quantum dots during the growth of a GaAs encapsulation layer. Journal of Crystal Growth, 2008, 310, 536-540.	1.5	3

#	Article	IF	CITATIONS
469	Electronic structure properties of the In(Ga)As/GaAs quantum dot–quantum well tunnel-injection system. Semiconductor Science and Technology, 2009, 24, 085011.	2.0	3
470	Quantum well infrared photodetectors hardiness to the nonideality of the energy band profile. Journal of Applied Physics, 2010, 107, .	2.5	3
471	Structural analysis of site-controlled InAs/InP quantum dots. Journal of Crystal Growth, 2011, 334, 37-39.	1.5	3
472	Last advances in Yb3+doped CaF 2 ceramics synthesis. , 2011, , .		3
473	Addition of Si-Containing Gases for Anisotropic Etching of Ill–V Materials in Chlorine-Based Inductively Coupled Plasma. Japanese Journal of Applied Physics, 2011, 50, 08JE02.	1.5	3
474	Mechanism of Ohmic Cr/Ni/Au contact formation on p-GaN. Journal of Vacuum Science and Technology B:Nanotechnology and Microelectronics, 2012, 30, 022205.	1.2	3
475	Resonant TE Transmission Through a Continuous Metal Film: Perspectives for Low-Loss Plasmonic Elements. Plasmonics, 2013, 8, 829-833.	3.4	3
476	Bonding mechanism of a yttrium iron garnet film on Si without the use of an intermediate layer. Applied Physics Letters, 2014, 105, 141601.	3.3	3
477	Nanoparticle Electrical Analysis and Detection with a Solid-state Nanopore in a Microfluidic Device. Procedia Engineering, 2016, 168, 1475-1478.	1.2	3
478	Locally measuring the adhesion of InP directly bonded on sub-100 nm patterned Si. Nanotechnology, 2016, 27, 115707.	2.6	3
479	Chemical lift-off and direct wafer bonding of GaN/InGaN P–I–N structures grown on ZnO. Journal of Crystal Growth, 2016, 435, 105-109.	1.5	3
480	Effect of Dot-Height Truncation on the Device Performance of Multilayer InAs/GaAs Quantum Dot Solar Cells. IEEE Journal of Photovoltaics, 2016, 6, 584-589.	2.5	3
481	Voided Ge/Si Platform to Integrate III-V Materials on Si. ECS Transactions, 2019, 93, 81-85.	0.5	3
482	InAs/GaSb thin layers directly grown on nominal (0â€ [−] 0â€ [−] 1)-Si substrate by MOVPE for the fabrication of InAs FINFET. Journal of Crystal Growth, 2019, 510, 18-22.	1.5	3
483	Effects of nitrogen incorporation and thermal annealing on the optical and spin properties of GaPN dilute nitride alloys. Journal of Alloys and Compounds, 2020, 814, 152233.	5.5	3
484	Microstructure of GaAs thin films grown on glass using Ge seed layers fabricated by aluminium induced crystallization. Thin Solid Films, 2020, 694, 137737.	1.8	3
485	Experimental quantification of atomically-resolved HAADF-STEM images using EDX. Ultramicroscopy, 2021, 220, 113152.	1.9	3
486	Single-Electron Tunneling PbS/InP Heterostructure Nanoplatelets for Synaptic Operations. ACS Applied Materials & Interfaces, 2021, 13, 38450-38457.	8.0	3

#	Article	IF	CITATIONS
487	Nanoindentation investigation of solid-solution strengthening in III-V semiconductor alloys. International Journal of Materials Research, 2005, 96, 1237-1241.	0.8	3
488	Nanoindentation investigation of solid-solution strengthening in III-V semiconductor alloys. International Journal of Materials Research, 2022, 96, 1237-1241.	0.3	3
489	Extended defects in II-VI semiconductor heteroepitaxial layers grown on GaAs substrates of various orientations. Physica Status Solidi A, 1993, 138, 437-443.	1.7	2
490	Designing the relative impact of thickness/composition changes in selective area organometallic epitaxy for monolithic integration applications. , 0, , .		2
491	Plasticity of GaAs(011) at room temperature under concentrated load. Philosophical Magazine Letters, 2001, 81, 527-535.	1.2	2
492	Onset of plasticity in a $l \pounds$ = 5 GaAs compliant structure. Philosophical Magazine Letters, 2001, 81, 813-822.	1.2	2
493	Influence of the twist angle on the plasticity of the GaAs compliant substrates realized by wafer bonding. Journal of Physics Condensed Matter, 2002, 14, 12967-12974.	1.8	2
494	Strength Enhancement of Compensated Strained InP/AlP Superlattice. Physica Status Solidi A, 2002, 189, 175-181.	1.7	2
495	Improvement of heteroepitaxial growth by the use of twist-bonded compliant substrate: Role of the surface plasticity. Journal of Electronic Materials, 2003, 32, 861-867.	2.2	2
496	Polarity influence on the nanoindentation response of GaAs. Physica Status Solidi C: Current Topics in Solid State Physics, 2005, 2, 2004-2009.	0.8	2
497	Modulation spectroscopy characterization of InAs/GaInAsP/InP quantum dash laser structures. , 2007, 6481, 52.		2
498	Tolerance to Optical Feedback of 10 GBPs Quantum-Dash Based Lasers Emitting at 1.55 μm. , 2007, , .		2
499	Heterostructure formation in nanowhiskers via diffusion mechanism. Technical Physics Letters, 2008, 34, 750-753.	0.7	2
500	Nanoindentation response of a thin InP membrane. Journal Physics D: Applied Physics, 2008, 41, 074003.	2.8	2
501	Localisation of silicon nanowires grown by UHV-CVD in (111)-oriented apertures opened in Si (001). IOP Conference Series: Materials Science and Engineering, 2009, 6, 012015.	0.6	2
502	Structure of annealed nanoindentations in n- and p-doped (001)GaAs. Journal of Applied Physics, 2009, 106, .	2.5	2
503	Direct FIB fabrication and integration of "single nanopore devices―for the manipulation of macromolecules. Materials Research Society Symposia Proceedings, 2009, 1191, 78.	0.1	2
504	Optically Active Defects in an InAsP/InP Quantum Well Monolithically Integrated on SrTiO3 (001). Materials Research Society Symposia Proceedings, 2010, 1252, 1.	0.1	2

#	Article	IF	CITATIONS
505	Nano-Patterning of Graphene Structures Using Highly Focused Beams of Gallium Ions. Materials Research Society Symposia Proceedings, 2010, 1259, 1.	0.1	2
506	Structure and Magnetism of Orthorhombic Epitaxial FeMnAs. Crystal Growth and Design, 2013, 13, 4279-4284.	3.0	2
507	Aberration corrected STEM to study an ancient hair dyeing formula. AIP Conference Proceedings, 2014, , ,	0.4	2
508	Investigation on Mn doping of Ge nanowires for spintronics. Physica Status Solidi C: Current Topics in Solid State Physics, 2014, 11, 315-319.	0.8	2
509	Instrumented nanoindentation and scanning electron transmission microscopy applied to the study of the adhesion of InP membranes heteroepitaxially bonded to Si. EPJ Applied Physics, 2014, 65, 20702.	0.7	2
510	Simultaneous growth of GaN/AlGaN quantum wells on c-, a-, m-, and (20.1)-plane GaN bulk substrates obtained by the ammonothermal method: Structural studies. Journal of Crystal Growth, 2015, 414, 87-93.	1.5	2
511	Nanostructure and luminescence properties of amorphous and crystalline ytterbium–yttrium oxide thin films obtained with pulsed reactive crossed-beam deposition. Journal of Materials Science, 2015, 50, 1267-1276.	3.7	2
512	Surface effects on exciton diffusion in non polar ZnO/ZnMgO heterostructures. Journal of Physics Condensed Matter, 2017, 29, 485706.	1.8	2
513	Controlled Dislocations Injection in N/P Hg1â^'xCdxTe Photodiodes by Indentations. Journal of Electronic Materials, 2019, 48, 6108-6112.	2.2	2
514	Effect of sintering germanium epilayers on dislocation dynamics: From theory to experimental observation. Acta Materialia, 2020, 200, 608-618.	7.9	2
515	Development of a cryogenic indentation tool with in situ optical observation, application to the mechanical characterization of Il–VI semiconductors. Semiconductor Science and Technology, 2021, 36, 035015.	2.0	2
516	Temperature dependence of optical properties of InAs/InP quantum rod-nanowires grown on Si substrate. Journal of Luminescence, 2021, 231, 117814.	3.1	2
517	Fabrication and characterization of ZnO:Sb/n-ZnO homojunctions. Applied Physics A: Materials Science and Processing, 2021, 127, 1.	2.3	2
518	Engineering dislocations and nanovoids for high-efficiency III–V photovoltaic cells on silicon. AIP Conference Proceedings, 2020, , .	0.4	2
519	Structural, vibrational, and magnetic properties of self-assembled CoPt nanoalloys embedded in SrTiO3. Physical Review Materials, 2020, 4, .	2.4	2
520	A study of the strain distribution by scanning X-ray diffraction on GaP/Si for Ill–V monolithic integration on silicon. Journal of Applied Crystallography, 2019, 52, 809-815.	4.5	2
521	Atomic scale analyses of {b Z}-module defects in an NiZr alloy. Acta Crystallographica Section A: Foundations and Advances, 2018, 74, 647-658.	0.1	2
522	Heteroepitaxial growth of silicon on GaAs via low-temperature plasma-enhanced chemical vapor deposition. , 2019, , .		2

#	Article	IF	CITATIONS
523	Polarity-induced changes in the nanoindentation response of GaAs. Journal of Materials Research, 2004, 19, 131-136.	2.6	2
524	Addition of Si-Containing Gases for Anisotropic Etching of Ill–V Materials in Chlorine-Based Inductively Coupled Plasma. Japanese Journal of Applied Physics, 2011, 50, 08JE02.	1.5	2
525	Comparative Study on the Quality of Microcrystalline and Epitaxial Silicon Films Produced by PECVD Using Identical SiF4 Based Process Conditions. Materials, 2021, 14, 6947.	2.9	2
526	Transmission Electron Microscopy Studies of Lattice-Mismatched Semiconductor Heterostructures Used for Integrated Optoelectronic Devices. Solid State Phenomena, 1996, 51-52, 131-142.	0.3	1
527	Optical studies of ultrashort-period GaAs/AlAs superlattices grown on (In,Ga)As pseudosubstrate. Physical Review B, 1998, 58, R7540-R7543.	3.2	1
528	GaAsSbN: a material for 1.3-1.55 μm emission. , 0, , .		1
529	Plasticity of GaAs compliant substructures. Materials Science & Engineering A: Structural Materials: Properties, Microstructure and Processing, 2001, 309-310, 478-482.	5.6	1
530	Effect of the p+-GaAs contact layer doping level on the gradual degradation of InGaAs/AlGaAs pump lasers. EPJ Applied Physics, 2004, 27, 465-468.	0.7	1
531	Buried dislocation networks for the controlled growth of Ill–V semiconductor nanostructures. Journal of Crystal Growth, 2005, 275, e1647-e1653.	1.5	1
532	Stress-engineered orderings of self-assembled III-V semiconductor nanostructures. Physica Status Solidi C: Current Topics in Solid State Physics, 2005, 2, 1245-1250.	0.8	1
533	Electroabsorption spectroscopy of Geâ^•Si self-assembled islands. Journal of Applied Physics, 2005, 97, 083525.	2.5	1
534	Metal-insulator Transition and Magnetic Domains in (Ga,Mn)As Epilayers. Materials Research Society Symposia Proceedings, 2006, 941, 1.	0.1	1
535	Indium incorporation in In-richInxGa1â^'xAsâ^•GaAslayers grown by low-pressure metalorganic vapor-phase epitaxy and its influence on the growth of self-assembled quantum dots. Physical Review B, 2006, 73, .	3.2	1
536	InAs/InP Quantum Dash Based Electro Optic Modulator with Over 70 NM Bandwidth at 1.55 μM. , 2007, , .		1
537	Large intrinsic birefringence in zinc-blende based artificial semiconductors. Comptes Rendus Physique, 2007, 8, 1174-1183.	0.9	1
538	Influence of recapture on the emission statistics of short radiative lifetime quantum dots. Physica Status Solidi C: Current Topics in Solid State Physics, 2008, 5, 2520-2523.	0.8	1
539	A new way to integrate solid state nanopores for translocation experiments. Microelectronic Engineering, 2008, 85, 1311-1313.	2.4	1
540	Influence of surface reconstructions on the shape of InAs quantum dots grown on InP(001). , 2008, , .		1

#	Article	IF	CITATIONS
541	Surface-plasmon distributed-feedback mid-infrared quantum cascade lasers based on hybrid plasmon/air-guided modes. , 2008, , .		1
542	Exploration of the Ultimate Patterning Potential Achievable with Focused Ion Beams. Materials Research Society Symposia Proceedings, 2008, 1089, 30101.	0.1	1
543	InP nanowires grown on Silicon and SrTiO <inf>3</inf> by VLS assisted MBE. , 2008, , .		1
544	Semiconductor nanowires in InP and related material systems: MBE growth and properties. , 2008, , .		1
545	Recent developments of InP-based quantum dashes for directly modulated lasers and semiconductor optical amplifiers. Proceedings of SPIE, 2008, , .	0.8	1
546	Doping influence on the nanoindentation response of GaAs. Physica Status Solidi C: Current Topics in Solid State Physics, 2009, 6, 1841-1846.	0.8	1
547	Optimization of 1550nm InAs/InP Quantum Dash and Quantum Dot based semiconductor optical amplifier. , 2009, , .		1
548	Columnar Quantum Dashes for polarization insensitive semiconductor optical amplifiers. , 2009, , .		1
549	Single photon sources using InAs/InP quantum dots. Proceedings of SPIE, 2009, , .	0.8	1
550	Quantum optics with single nanowire quantum dots. , 2010, , .		1
551	Tailoring nanopores for efficient sensing of different biomolecules. Materials Research Society Symposia Proceedings, 2010, 1253, 33.	0.1	1
552	Nanowires for quantum optics. , 2010, , .		1
553	New generation of Distributed Bragg Reflectors based on BAIN/AIN structures for deep UV-optoelectronic applications. , 2011, , .		1
554	Direct epitaxial growth of InP based heterostructures on SrTiO3/Si(001) crystalline templates. Microelectronic Engineering, 2011, 88, 469-471.	2.4	1
555	Tuning the structural properties of InAs nanocrystals grown by molecular beam epitaxy on silicon dioxide. Journal of Crystal Growth, 2011, 321, 1-7.	1.5	1
556	Stored elastic energy influence on the elastic–plastic transition of GaAs structures. Journal of Materials Research, 2012, 27, 177-181.	2.6	1
557	Recent advances in development of vertical-cavity based short pulse source at 1.55 μm. Frontiers of Optoelectronics, 2014, 7, 1-19.	3.7	1
558	Nanoscale Surface and Sub-Surface Chemical Analysis of SiGe Nanowires. Microscopy and Microanalysis, 2014, 20, 2052-2053.	0.4	1

#	Article	IF	CITATIONS
559	Probing the electronic properties of CVD graphene superlattices. , 2016, , .		1
560	First orientation-patterned GaSb ridge waveguides fabrication and preliminary characterization for frequency conversion in the mid-infrared. Proceedings of SPIE, 2016, , .	0.8	1
561	Nanoselective area growth of defect-free thick indium-rich InGaN nanostructures on sacrificial ZnO templates. Nanotechnology, 2017, 28, 195304.	2.6	1
562	High structural and optical quality of III-V-on-Si 1.2 nm-thick oxide-bonded hybrid interface. Microelectronic Engineering, 2018, 192, 25-29.	2.4	1
563	Composition and Face Polarity Influences on Mechanical Properties of (111) Cd1â^'yZnyTe Determined by Indentation. Journal of Electronic Materials, 2019, 48, 6985-6990.	2.2	1
564	Gate length dependent transport properties of in-plane core-shell nanowires with raised contacts. Nano Research, 2020, 13, 61-66.	10.4	1
565	Measuring the surface bonding energy: A comparison between the classical double-cantilever beam experiment and its nanoscale analog. AIP Advances, 2020, 10, 045006.	1.3	1
566	Efficient Electrical Transport Through Oxideâ€Mediated InPâ€onâ€Si Hybrid Interfaces Bonded at 300 °C. Physica Status Solidi (A) Applications and Materials Science, 2021, 218, 2000317.	1.8	1
567	Relaxation mechanism of GaP grown on 001 Si substrates: influence of defects on the growth of AlGaP layers on GaP/Si templates. Philosophical Magazine, 2021, 101, 2189-2199.	1.6	1
568	Highly linear polarized emission at telecom bands in InAs/InP quantum dot-nanowires by geometry tailoring. Nanoscale, 2021, 13, 16952-16958.	5.6	1
569	Transformation de phase dans un film de germanium amorphe induite par nano-indentation. Materiaux Et Techniques, 2005, 93, 257-262.	0.9	1
570	Chemical nature of the anion antisite in dilute phosphide <mml:math xmlns:mml="http://www.w3.org/1998/Math/MathML"> <mml:mrow> <mml:mi>GaA</mml:mi> <mml:msub> <mml: mathvariant="normal">s <mml:mrow> <mml:mn> 1 </mml:mn> <mml:mo>â^^</mml:mo> <mml:mi>xmathvariant="normal">P</mml:mi> <mml:mi>x</mml:mi> </mml:mrow></mml: </mml:msub> </mml:mrow> alloy</mml:math 	mi ml 2mai > <td>۱ml:mrow><!--۱</td--></td>	۱m l: mrow> ۱</td
571	grown at low temperature. Physical Review Materials, 2018, 2, . Towards polarization insensitive semiconductor optical amplifiers using InAs/GaAs columnar quantum dots. , 2008, , .		1
572	Growth of III-Arsenide/Phosphide Nanowires by Molecular Beam Epitaxy. , 2011, , 68-88.		1
573	(Invited) Tensile Strain Engineering and Defects Management in GeSn Laser Cavities. ECS Transactions, 2020, 98, 61-68.	0.5	1
574	Capturing the Effects of Free Surfaces on Threading Dislocation Density Reduction. ECS Transactions, 2020, 98, 527-532.	0.5	1
575	In-plane InGaAs/Ga(As)Sb nanowire based tunnel junctions grown by selective area molecular beam epitaxy. Nanotechnology, 2022, 33, 145201.	2.6	1
576	Photo-Activated Phosphorescence of Ultrafine ZnS:Mn Quantum Dots: On the Lattice Strain Contribution. Journal of Physical Chemistry C, 2022, 126, 1531-1541.	3.1	1

#	Article	IF	CITATIONS
577	Optical and structural properties of 1.3 \hat{l} /4m emitting InAs/GaAs quantum dots grown by LP-MOVPE as a function of the re-growth temperature. , 0, , .		0
578	Wafer bonded all-optical switching devices. , 0, , .		0
579	Wet thermal oxidation of AlInAs and AlAsSb alloys lattice-matched to InP. , 0, , .		0
580	Cubic phase gallium nitride epitaxially formed on GaAs or GaInAs at low temperature with a NH3 DECR plasma. , 0, , .		0
581	Low damage dry-etched grating on a MQW active layer and dislocation-free InP regrowth for 1.55 μm complex-coupled DFB lasers fabrication. , 0, , .		0
582	Morphological and Compositional Instabilities of Strained and Unstrained Alloy Layers. Materials Research Society Symposia Proceedings, 1999, 583, 315.	0.1	0
583	Ultrafast saturable absorber device with heavy-ion irradiated quantum wells for high bit-rate optical regeneration at 1.55 \hat{l} /4m. , 0, , .		0
584	Detailed comparison of GalnNAs/GaAs and GalnNAs/GaNAs/GaAs quantum wells emitting near 1.3 μm wavelength. , 0, , .		0
585	Phase separation and superlattice formation by spontaneous vertical composition modulation in GaAs1â^'xNx/GaAs. Physica Status Solidi C: Current Topics in Solid State Physics, 2003, 0, 2749-2752.	0.8	0
586	MOVPE growth and characterization of long-wavelength emitting quantum dots based lasers at 300 K. , 0, , .		0
587	Piezoelectric InGaAs/GaAs/AlGaAs quantum well lasers grown on (111)A GaAs by metalorganic vapor phase epitaxy. , 0, , .		0
588	Material and optical properties of GaAs grown on (001) Ge/Si pseudo-substrate. Materials Research Society Symposia Proceedings, 2004, 809, B2.4.1.	0.1	0
589	Thermal stability of ion-irradiated InGaAs with subpicosecond carrier lifetime. , 2004, , .		0
590	An indentation method to measure the CRSS of semiconducting materials at elevated temperature. Materials Science & Engineering A: Structural Materials: Properties, Microstructure and Processing, 2005, 400-401, 451-455.	5.6	0
591	Conservative indentation flow throughout thin (011) InP foils. Journal of Materials Science, 2005, 40, 3809-3811.	3.7	0
592	Deviation of the mechanical response of Wall-patterned (001) GaAs Surface: a central-plastic-zone criterion. Materials Research Society Symposia Proceedings, 2005, 904, 1.	0.1	0
593	Determination of In(Ga)As/GaAs quantum dot composition profile. AIP Conference Proceedings, 2005, , ·	0.4	0
594	Indentation Crystallization and Phase Transformation of Amorphous Germanium. Materials Research Society Symposia Proceedings, 2005, 904, 1.	0.1	0

#	Article	IF	CITATIONS
595	InAs/InP(001) quantum dots and quantum sticks grown by MOVPE: shape, anisotropy and formation process. Physica Status Solidi C: Current Topics in Solid State Physics, 2006, 3, 3928-3931.	0.8	0
596	Towards a mid-infrared polaron laser using InAs/GaAs self-assembled quantum dots. Physica Status Solidi (B): Basic Research, 2006, 243, 3895-3899.	1.5	0
597	Synthesis and Optical Properties of Silicon Oxide Nanowires. Materials Research Society Symposia Proceedings, 2006, 958, 1.	0.1	Ο
598	Microphotoluminescence around 1.5 μm from a single InAs/InP(001) quantum dot grown by MOVPE , 2006, , .		0
599	Strong linear polarization induced by a longitudinal magnetic field in II-VI semimagnetic semiconductor layers. Physical Review B, 2006, 74, .	3.2	Ο
600	Mechanical response of a single and released InP membrane. Materials Research Society Symposia Proceedings, 2007, 1049, 1.	0.1	0
601	Processing of InP-Based Shallow Ridge Laser Waveguides Using a HBr ICP Plasma. Indium Phosphide and Related Materials Conference (IPRM), IEEE International Conference on, 2007, , .	0.0	Ο
602	InAs/InP(001) Quantum Dots And Quantum Sticks Grown By MOVPE: Shape, Anisotropy And Formation Process. AIP Conference Proceedings, 2007, , .	0.4	0
603	Photonic crystal nanolasers with controlled spontaneous emission. Proceedings of SPIE, 2008, , .	0.8	0
604	Tuning InAs/InP(001) quantum dot emission from 1.55 to 2 \hat{l} 4m by varying cap-layer growth rate in metalorganic vapor phase epitaxy. , 2008, , .		0
605	One step Nano Selective Area Growth of localized InAs/InP quantum dots for single photon source applications. , 2008, , .		Ο
606	Monolithic integration of InP based heterostructures on silicon using crystalline Gd <inf>2</inf> O <inf>3</inf> buffers. , 2008, , .		0
607	InAsP/InP(001) quantum dots emitting at 1.55 \hat{l} ¼m grown by metalorganic vapor phase epitaxy. , 2008, , .		Ο
608	Mechanism of anisotropy during inductively coupled plasma (ICP) etching of inp-based heterostructures for the fabrication of photonic devices. , 2008, , .		0
609	Dipole orientation in a Quantum Rod. , 2008, , .		Ο
610	Epitaxial growth and picosecond carrier dynamics at 1.55µm of GalnAs/GalnNAs superlattices. , 2009, , .		0
611	One Step Nano-Selective Area Growth of Localized InAs/InP Quantum Dots For Single Photon Source Applications. Materials Research Society Symposia Proceedings, 2009, 1228, 120701.	0.1	0
612	Mid/far-infrared semiconductor devices exploiting plasmonic effects. Proceedings of SPIE, 2009, , .	0.8	0

#	Article	IF	CITATIONS
613	Challenges and Opportunities for Focused Ion Beam Processing at the Nano-scale. Microscopy and Microanalysis, 2009, 15, 320-321.	0.4	0
614	Nanoindentation-induced structural phase transformations in crystalline and amorphous germanium. International Journal of Nano and Biomaterials, 2009, 2, 91.	0.1	0
615	Effects of substrates and catalysts compositions on the crystalline quality of InP Nanowires grown on SrTiO3 (001), Si(001) and InP (111). Materials Research Society Symposia Proceedings, 2010, 1258, 1.	0.1	0
616	Optical and structural properties of INP nanowires grown on silicon substrate. , 2010, , .		0
617	Confined and Guided Vapor–Liquid–Solid Catalytic Growth of Silicon Nanoribbons: From Nanowires to Structured Silicon-on-Insulator Layers. Engineering Materials, 2011, , 67-89.	0.6	Ο
618	Selective growth of site-controlled Quantum Dots. , 2011, , .		0
619	Kinetics and Statistics of Vapor-Liquid-Solid Growth of III-V Nanowires. Materials Research Society Symposia Proceedings, 2012, 1408, 81.	0.1	Ο
620	Quantum efficiency of InAs/InP nanowire heterostructures grown on silicon substrates. Physica Status Solidi - Rapid Research Letters, 2013, 7, 878-881.	2.4	0
621	Improvement of the oxidation interface in an Al <scp>G</scp> a <scp>A</scp> s/ <scp>A</scp> l _{<i>x</i>} <scp>O</scp> _{<i>y</i>} waveguide structure by using a Ga <scp>A</scp> s/ <scp>A</scp> l <scp>A</scp> s superlattice. Physica Status Solidi (A) Applications and Materials Science. 2013. 210. 1171-1177.	1.8	0
622	Control of heterointerface and strain mapping in Au catalyzed axial Si-Si1-xGex nanowires. Materials Research Society Symposia Proceedings, 2014, 1707, 37.	0.1	0
623	Wafer bonding of Si for hybrid photonic devices. Materials Research Society Symposia Proceedings, 2014, 1748, 1.	0.1	Ο
624	Plasticity and Fracture of InP/Si Substructures. Materials Science Forum, 0, 783-786, 1628-1633.	0.3	0
625	Direct bonding of YIG film on Si without intermediate layer. , 2014, , .		Ο
626	Electrical transport across the heterointerface of InP membranes bonded oxide-free on Si. , 2014, , .		0
627	Photoluminescence polarization and piezoelectric properties of InAs/InP quantum rod-nanowires. , 2014, , .		Ο
628	Investigation of new approaches for InGaN growth with high indium content for CPV application. AIP Conference Proceedings, 2015, , .	0.4	0
629	Local probing of the interfacial strength in InP/Si substructures. MRS Advances, 2016, 1, 779-784.	0.9	0
630	(Invited) Locally Measuring the Adhesion of InP Membranes Directly Bonded on Silicon. ECS Transactions, 2016, 75, 169-176.	0.5	0

#	Article	IF	CITATIONS
631	Publisher's Note: Interplay between tightly focused excitation and ballistic propagation of polariton condensates in a ZnO microcavity [Phys. Rev. B92, 235308 (2015)]. Physical Review B, 2016, 93, .	3.2	0
632	Enhanced sputtering of Ge nanowires under synergetic effect of Mn ion and electron beams. Results in Physics, 2017, 7, 3813-3814.	4.1	0
633	Quantum cascade lasers grown on silicon. , 2018, , .		0
634	Ultra-Low Threshold CW Lasing in Tensile Strained GeSn Microdisk Cavities. , 2019, , .		0
635	High density InAlAs/GaAlAs quantum dots as an efficient enhanced Kerr material for transverse non-linear optics in microcavities. , 2005, , .		0
636	Quality Factor of Micropillar Cavity. , 2006, , .		0
637	Indentation behaviour of (011) thin films of III–V semiconductors: polarity effect differences between GaAs and InP. International Journal of Materials Research, 2006, 97, 1230-1234.	0.3	0
638	Advances in fluoride-based ceramic laser media. , 2007, , .		0
639	Towards A Mid-Infrared Polaron Laser Using InAs/GaAs Self-Assembled Quantum Dots. AIP Conference Proceedings, 2007, , .	0.4	0
640	Surface-Plasmons on Structured Metallic Surfaces: Theoretical Analysis, Applications to Mid-Infrared Quantum Cascade Lasers and a-SNOM Survey. , 2008, , .		0
641	Surface emitting photonic crystal mid-infrared quantum cascade lasers. , 2009, , .		0
642	Growth of III-Arsenide/Phosphide Nanowires by Molecular Beam Epitaxy. , 2011, , 68-88.		0
643	Gravure hélicon de l'InP en plasma HBr. Morphologie et caractérisation des défauts de surface. Journal De Physique III, 1995, 5, 467-481.	0.3	0
644	III-V Nanowires on Silicon: a possible route to Si-based tandem solar cells. , 2017, , .		0
645	Large angle twist-bonded compliant substrates for the epitaxy of lattice mismatched III-V semiconductors. , 2018, , 193-196.		0
646	Z-modules in crystallography: structures and defects. Acta Crystallographica Section A: Foundations and Advances, 2018, 74, e103-e104.	0.1	0
647	TEM determination of the local concentrations of substitutional and interstitial Mn and antisite defects in ferromagnetic GaMnAs. , 2005, , 147-150.		0
648	Nano-FIB from Research to Applications — a European Scalpel for Nanosciences. Springer Proceedings in Physics, 2008, , 431-440.	0.2	0

#	Article	IF	CITATIONS
649	Defects management in the gain media of GeSn micro-disk lasers. , 2020, , .		0
650	Indentation behaviour of (011) thin films of III–V semiconductors: polarity effect differences between GaAs and InP. International Journal of Materials Research, 2022, 97, 1230-1234.	0.3	0